Ingested double-stranded RNA and their mobile RNA derivatives have different requirements for gene silencing in *C. elegans*.

Pravrutha Raman, Soriayah M Zaghab, Edward C Traver, and Antony M Jose*

Department of Cell Biology and Molecular Genetics, University of Maryland, College Park, MD-20742.

Running Title: Feeding RNAi mechanisms

Keywords: Feeding RNAi, repetitive transgenes, Argonaute

*Corresponding author: Antony M Jose, Rm 2136, Bioscience Research Building (Bldg #413), University of Maryland, College Park, MD-20742. Phone no: 301-405-7028. E-mail: amjose@umd.edu

ABSTRACT

Double-stranded RNA (dsRNA) can cause specific gene silencing upon ingestion in many invertebrates and is being developed as a pesticide to target essential genes in animal pests. Silencing by ingested dsRNA is best understood in the worm *C. elegans*, where ingested dsRNA is recruited into the RNA interference (RNAi) pathway by the dsRNA-binding protein RDE-4 for eventual gene silencing by Argonaute proteins. Although silencing is thought to rely on both the ingested dsRNA and on additional dsRNA-derived RNAs called mobile RNAs that are transported between cells, the specific forms of RNA that enter different tissues and the proteins they engage to cause silencing are unclear. We found that when RDE-4 was expressed at high levels within a somatic tissue, silencing by ingested dsRNA could occur in *rde-4(-)* somatic tissues but not in the *rde-4(-)* germline. Consistent with the spread of dsRNA-derived mobile RNAs between cells, silencing was more efficient in *rde-4(-)* cells located near *rde-4(+)* cells. Surprisingly, silencing by mobile RNAs derived from ingested dsRNA could bypass the requirement for a nuclear Argonaute that both ingested dsRNA and mobile RNAs derived from neuronal dsRNA require for silencing the same target gene. Furthermore, silencing by mobile RNAs could bypass inhibition of silencing within a tissue that can be caused by expression from repetitive DNA in that tissue. These results identify possible mechanisms that animals can use to evade RNAi and suggest that mobile RNA derivatives of ingested dsRNA can bypass these resistance mechanisms and cause gene silencing.

INTRODUCTION

Killing animals by feeding them double-stranded RNA (dsRNA) that matches an essential gene is a powerful approach to control animal pests. For example, expression of long dsRNA in potato plants was recently used to control populations of Colorado potato beetle that feed on these plants (Zhang *et al.* 2015). This approach to pest control relies on the ability of many insects and parasitic nematodes to ingest long dsRNA and use it to silence genes of matching sequence (Baum *et al.* 2007; Mao *et al.* 2007; reviewed in Koch and Kogel 2014) through RNA interference (RNAi). However, the mechanisms of gene silencing by ingested dsRNA are not well understood, making it difficult to anticipate resistance mechanisms and therefore design effective drugs.

Silencing of genes by feeding animals long dsRNA was first demonstrated in the nematode *C. elegans* (Timmons and Fire 1998) and it remains the best animal model for understanding this process called feeding RNAi. In *C. elegans*, ingested dsRNA enters the animal through the intestine and can be delivered into the fluid-filled body cavity that all tissues are exposed to without entry into the cytosol of intestinal cells (Jose *et al.* 2009; Calixto *et al.* 2010; Hinas *et al.* 2012). Entry into the cytosol of any cell requires a dsRNA-selective importer SID-1 (Winston *et al*. 2002) – a conserved protein with homologs in many insects (Tomoyasu *et al.* 2008). Upon entry into cells, silencing by dsRNA is thought to occur through the canonical RNAi pathway (reviewed in Grishok 2013). Long dsRNA is first bound by the dsRNA-binding protein RDE-4, which recruits the endonuclease DCR-1 to generate short dsRNAs (Tabara *et al.* 2002; Parker *et al.* 2006). One strand of this short dsRNA duplex is used as a guide by the primary

Argonaute RDE-1 to identify mRNAs of matching sequence and to recruit RNA-dependent RNA polymerases (RdRPs) to the mRNA. RdRPs then synthesize numerous secondary small RNAs that are used for potent gene silencing within the cytosol by cytosolic Argonautes and/or within the nucleus by nuclear Argonautes. In addition to using long dsRNA for silencing, cells can also generate mobile RNAs (RNAs that can move between cells) derived upon processing of ingested dsRNA within muscle cells that express the dsRNA-binding protein RDE-4 (Jose *et al.* 2011; Blanchard *et al.* 2011) or the putative nucleotidyltransferase MUT-2 (Jose *et al.* 2011). Whether other tissues can make such dsRNA-derived mobile RNAs and whether both ingested long dsRNAs and its mobile RNA derivatives require the same proteins for silencing a gene is unknown.

Here, we show that high levels of RDE-4 in muscle cells, intestinal cells, hypodermal cells, or neurons can all enable generation of mobile RNAs derived from ingested dsRNA in *C. elegans* and can silence other somatic tissues but not the germline. Furthermore, silencing in somatic tissues by these mobile RNAs can be distinguished from silencing by ingested dsRNA. Specifically, unlike ingested dsRNA, their mobile RNA derivatives can bypass the requirement for the nuclear Argonaute NRDE-3 to silence the hypodermal gene *bli-1* and can overcome the inhibition of silencing within a tissue caused by expression from repetitive transgenes in that tissue.

MATERIALS AND METHODS

Worm Strains

All strains were cultured on Nematode Growth Medium (NGM) plates seeded with 100 *μ*l OP50 at 20ºC and mutant combinations were generated using standard methods (Brenner 1974). All strains used are listed in Supplemental Material.

Balancing loci

Integrated transgenes expressing *gfp* were used to balance mutations in heterozygous animals. Progeny of heterozygous animals were scored as homozygous mutants if they lacked both copies of the transgene. The *rde-4(ne301)* allele on Chr III was balanced by *juIs73*. About 99% (153/155) progeny of *rde-4(ne301)/juIs73* that lacked fluorescence were found to be homozygous *rde-4(ne301)* animals either by Sanger sequencing (96) or by resistance to *pos-1* RNAi (59).

Transgenesis

To make strains, N2 gDNA was used (unless otherwise specified) as a template to amplify promoter or gene regions. To amplify *gfp* to be used as a coinjection marker a plasmid containing cytoplasmic *gfp* was used as a template (unless otherwise specified). All PCR reactions were performed with Phusion Polymerase (New England Biolabs- NEB), unless otherwise specified, according to the manufacturer's recommendations and the final fusion products were purified using PCR Purification Kit (Qiagen).

Plasmids

The plasmid pJM6 (made by Julia Marré, Jose lab) was used to make *Si[Pnas-9::rde-4(+)::rde-4 3'UTR]*. The *nas-9* promoter (*Pnas-9*) was amplified using primers P49 and P50 and *rde-4(+)::rde-4 3'UTR* was amplified using primers P54 and P4. The two PCR products were used as templates to generate the *Pnas-9::rde-4(+)::rde-4 3'UTR* fusion product with primers P52 and P53. This fused product was purified (QIAquick PCR Purification Kit, Qiagen) and cloned into pCFJ151 using the SbfI and SpeI restriction enzymes (NEB) to generate pJM6.

The plasmid pYC13 (made by Yun Choi, Jose lab) is a derivative of pUC::unc-119_sgRNA with a different sgRNA (gift from John Calarco, Addgene plasmid # 46169)) All other plasmids were as described earlier (pHC448 (Jose *et al*. 2011), pPD95.75 (gift from Andrew Fire, Addgene plasmid # 1494), pBH34.21 (Harfe and Fire 1998), pCFJ151 (Semple *et al.* 2012), pCFJ601 (Semple *et al.* 2012), pMA122 (Semple *et al.* 2012), pGH8 (Semple *et al.* 2012), pCFJ90 (Semple *et al.* 2012), pCFJ104 (Semple *et al.* 2012), pL4440 (Timmons and Fire 1998), pHC183 (Jose *et al*. 2009) and pGC306 (a gift from Jane Hubbard, Addgene plasmid # 19658)).

Genome editing

To generate *bli-1* null mutants, Cas9-based genome editing using a co-conversion strategy was used (Arribere *et al*. 2014). Guide RNA for *bli-1* was amplified from pYC13 using primer P56 and P57 and guide RNA for co-conversion of *dpy-10* was amplified from pYC13 using P58 and P57. The amplified guides were purified (PCR Purification Kit, Qiagen) and tested in vitro for cutting efficiency (Cas9, NEB). For injection into animals, homology template for repair (repair template) was amplified from N2 gDNA

using Phusion polymerase and gene specific primers. P59 and P60 was used to amplify a region immediately outside the 5' region of *bli-1* and P61 and P62 was used to amplify a region immediately outside the 3' region of *bli-1* using Phusion Polymerase (NEB). The two PCR products were used as templates to generate the repair template with primers P63 and P64 using Phusion Polymerase (NEB) and the fused product was purified (PCR Purification Kit, Qiagen). Homology template for *dpy-10* was a single-stranded DNA oligo (P65). Animals were injected with 3.5pmol/μl of *bli-1* guide RNA, 2.4pmol/μl of *dpy-10* guide RNA, 0.06pmol/μl of *bli-1* homology repair template, 0.6pmol/μl of *dpy-10* homology repair template and 1.6pmol/μl of Cas-9 protein (NEB). Resulting progeny animals were analyzed as described in Figure S6.

Feeding RNAi

RNAi experiments were performed on RNAi plates (NGM plates supplemented with 1 mM IPTG (Omega Bio-Tek) and 25μg/ml Carbenicillin (MP Biochemicals)) at 20ºC.

One generation or F1-only feeding RNAi. A single L4 or young adult (1 day older than L4) animal (P0) was placed on an RNAi plate seeded with 5μl of OP50 *E. coli* and allowed to lay eggs. After 1 day, by when most of the OP50 *E. coli* was eaten, the P0 animal was removed, leaving the F1 progeny. 100μl of an overnight culture of RNAi food (*E. coli* which express dsRNA against a gene) was added to the plate. Two or three days later, the F1 animals were scored for gene silencing by measuring gene-specific defects (See Table S1). All RNAi *E. coli* clones were from the Ahringer library (Kamath *et al.* 2003) and generously supplied by Iqbal Hamza, with the exception of *DsRed* and *unc-54* RNAi, which was made by cloning a fragment of *DsRed* and *unc-54* DNA,

respectively, into pL4440 and transforming into HT115(DE3) *E. coli* cells. Control RNAi by feeding *E. coli* containing the empty dsRNA-expression vector (pL4440), which does not produce dsRNA against any gene, was done in parallel with all RNAi assays.

Intensity of L4 animals fed dsRNA against *gfp* in was measured using Image J (NIH). Animals with an intensity of >6000(a.u.) in a fixed area within the gut immediately posterior to the pharynx were considered not silenced. Based on this criteria, 91.7% of wild-type animals and a 100% of animals expressing *DsRed* in the muscle (*Ex[Pmyo-3::DsRed]*) showed silencing. In these silenced animals intensity of *gfp* was measured from below the pharynx to the end of the vulva and the background intensity for the same area was measured for each animal. The intensity of *gfp* for the area after background subtraction was plotted for each worm (Figure 4E).

Two generations or P0 & F1 Feeding RNAi. The experiments in Figures 4-7 (except Figure 4A, Figure 6D) and Figures S1, S3, S4, and S7 (except Figure S4A) were performed by feeding both the P0 and F1 generations, as described earlier (Jose *et al.* 2009). Control RNAi was done in parallel with all RNAi assays. Three or four days after P0 animals were subjected to RNAi, the F1 animals were scored for gene silencing by measuring gene-specific defects (See Table S1).

No difference in gene silencing was observed between F1-only feeding RNAi and P0 & F1 feeding RNAi for *rde-4* mutants with tissue-specific rescue. For each RNAi experiment testing *rde-4* function, feeding of N2 and WM49 was performed alongside as controls. In the case of Figure 7E (*rde-4(-); Is[myo-3::rde-4(+)::rde-4 3'UTR; Ex[Pnas-9::gfp::unc-54 3'UTR]*) and Figure 5 (*act-5* feeding RNAi of *rde-4(-); Si[nas-9::rde-*

4(+)::rde-4 3'UTR; Ex[Pnas-9::gfp::unc-54 3'UTR]), L4 animals were scored a day after control L4 animals because these animals grew slower than control animals.

Mosaic Analyses

Animals with an integrated *Psur-5::sur-5::gfp* in an *rde-4(-)* background that in addition have *rde-4(+)* DNA in some cells marked by nuclear-localized *DsRed* expression (a single extrachromosomal array with *Psur-5::rde-4(+)* and *Psur-5::DsRed*) were analyzed. Animals were subjected to F1 only RNAi feeding of bacteria expressing no dsRNA (control RNAi) or bacteria expressing dsRNA against *gfp* (*gfp* RNAi). The resulting animals were imaged and those with dim *gfp* expression or no detectable *gfp* expression in at least one intestinal nucleus were scored as silenced (Figure 3).

Scoring defects

For RNAi treatments, the proportions of animals that displayed the reported mutant defects upon RNAi (see Table S1) were scored as "fraction silenced".

For *bli-1* defects upon RNAi as well as upon Cas9-based genome editing, the pattern of blister formation was scored. Each animal was partitioned into eight roughly equal sections (a to h) as shown in Figure 6A with the vulva being the mid point of the animal. Sections with >50% of their length covered by a blister were marked black and sections with a discontinuous blister were marked grey. Animals that did not follow the anterior more than posterior and dorsal more than ventral susceptibility pattern (a > b > c > d > e > f > g > h) were culled as variants for each genotype and the relative aggregate blister formation in each section among worms with altered susceptibility (Figure 6C, Figure S6E,G,H and S7B,D) were computed using a score of black = 1.0

and grey = 0.5 for each section of every worm. The computed values for each section in all worms of a strain were summed and normalized to the value of the highest section for that strain. To compare multiple strains, these values for each strain were multiplied by the fraction of worms that showed a blister in that strain. Using these measures of normalized relative aggregate blister formation among animals with variant susceptibility, we generated heat maps (Pavlidis *et al.* 2003), where black indicates highest frequency of blisters and white indicates the lowest frequency of blisters among the sections of all strains that are being compared.

Microscopy

Animals were immobilized in 5μl of 3mM levamisole, mounted on slides, and imaged using an AZ100 microscope (Nikon) at a fixed magnification under non-saturating conditions. Images being compared on any figure were adjusted identically using photoshop (levels adjustment) for display.

ImageJ (NIH) was used to generate merged images (Figure 3D, Figure 4D, and Figure S4G). The LUT was set from 0 (white) to 127 (magenta) for the red channel and from 0 (white) to 127 (green) for the green channel. One channel was then overlayed on the other with 50% opacity.

Semiquantitative RT-PCR

RNA from each strain was isolated from 50 L4-staged animals as described earlier (Devanapally *et al.* 2015). Primer, P66 was used to reverse transcribe the sense strand of *rde-4* and P67 was used to reverse transcribe the sense strand of *tbb-2*. The resulting cDNA was used as a template for PCR (30 cycles for both *rde-4* and *tbb-2*) using Taq

polymerase and gene-specific primers (P68 and P69 for *rde-4* and P70 and P71 for *tbb-2*). Intensity of the bands were quantified as described previously (Devanapally *et al.* 2015). The level of *rde-4(+)* mRNA in wild type was set as 1.0 and that in other strains with the *ne301* mutation were reported relative to that of wild type after subtracting the level of *rde-4(ne301)* mRNA in WM49 (0.3 in Figure S5).

Statistical Analyses

Error bars in all cases indicate 95% confidence intervals for single proportions calculated using Wilson's estimates with a continuity correction (Method 4 in Newcombe *et al.* 1998). Significance of differences between two strains or conditions was determined using pooled Wilson's estimates.

Data Availability

All strains are available upon request.

RESULTS

Tissue-specific rescue of *rde-4* enables silencing in somatic cells that lack *rde-4* expression but not in germline cells that lack *rde-4* expression

Evaluating the effects of mobile RNAs derived from ingested dsRNA requires approaches that restrict RNA processing to specific tissues. A common approach used for such restriction of a process is tissue-specific rescue of a mutant by driving expression of the corresponding wild-type gene under the control of a tissue-specific promoter. One caveat of this approach is that expression from a tissue-specific promoter may not be sufficiently tissue-specific and could result in low or even undetectable levels of expression in unintended tissues that are nevertheless sufficient to provide function. Thus, to interpret the results from a tissue-specific rescue experiment, we required that the promoters used be well-characterized and that the effect – in this case gene silencing – be tissue-restricted when using the promoter in at least one scenario. The tissue-specific rescue of *rde-1* has been demonstrated to cause tissue-restricted gene silencing in response to feeding RNAi (Qadota *et al.* 2007; Jose *et al.* 2011). Therefore, we required that a promoter enable tissue-specific gene silencing when used for tissue-specific rescue of *rde-1* before using it for tissue-specific rescue of *rde-4*.

We generated animals with tissue-specific rescues of *rde-4* by expressing *rde-4(+)* from a repetitive transgene under the control of tissue-specific promoters and assessed silencing in these animals in response to feeding RNAi against genes that function in different tissues. Specifically, we generated animals with rescue of *rde-4* in

body-wall muscles, intestine, hypodermis, or neurons and fed them dsRNA against target genes expressed in multiple tissues (Figure 1A, top). In all cases, ingested dsRNA enabled gene silencing in somatic tissues with *rde-4(+)* expression and in other somatic tissues that are expected to lack *rde-4* expression. Consistent with restricted expression from the tissue-specific promoters used, silencing of endogenous genes in the corresponding *rde-1(-)* animals with *rde-1(+)* expression under the same tissue-specific promoter was restricted to the tissue that expressed *rde-1(+)* (Figure 1A, bottom; Qadota *et al.* 2007; Jose *et al.* 2011). However, some silencing of ubiquitously expressed green fluorescent protein (*gfp*) in non-muscle tissues was observed even in *rde-1(-)* animals with *rde-1(+)* expressed in body-wall muscles (*Pmyo-3*) (Figure S1), reflecting either modest silencing of this exogenous gene by RDE-1-dependent mobile RNAs or weak misexpression in non-muscle tissues from the muscle-specific promoter. In general, these results suggest that unlike in the case of animals with tissue-specific *rde-1* rescue, in animals with tissue-specific *rde-4* rescue, expression of the wild-type gene in a somatic tissue is not required for silencing of an endogenous gene expressed in that tissue by feeding RNAi. In contrast, silencing of a gene expressed within the *rde-4(-)* germline was not detected when *rde-4(+)* was expressed in any somatic tissue (Figure 1A, top, grey bars). This difference between silencing of somatic genes and of germline genes could result from either tissue-specific or target gene-specific differences. To eliminate target differences, we examined the silencing of *gfp* expressed from the same promoter (*Pgtbp-1::gtbp-1::gfp*) in both somatic tissues and in the germline. In animals with *rde-4* rescue in a somatic tissue, silencing in response to

ingested dsRNA occurred within multiple somatic tissues but not within the germline (Figure 1B&C and Figure S2). Thus, either the germline does not import sufficient amounts of mobile RNAs produced after the processing of ingested dsRNA in a somatic tissue by RDE-4 or the germline RNAi machinery is unable to recognize and use such mobile RNA derivatives of ingested dsRNA.

In summary, analyses of animals with tissue-specific rescue of *rde-4* reveal that the generation of mobile RNAs derived from ingested dsRNA can occur in multiple somatic tissues and that these mobile RNAs can silence genes in other somatic tissues but not in the germline.

Somatic RDE-4 in parents cannot enable feeding RNAi in *rde-4(-)* progeny

Repetitive transgenes can sometimes result in expression within the germline despite the use of somatic promoters (e.g. heat shock promoter (Sheth *et al.* 2010)). Such misexpression within the germline and subsequent delivery of RDE-4 into progeny would complicate interpretation of silencing in animals with tissue-specific rescue of *rde-4*. Therefore, to test if such parental rescue is detectable, we expressed *rde-4(+)* in the body-wall muscle, hypodermis, or intestine of *rde-4(-)* animals and fed only their *rde-4(-)* progeny dsRNA against genes expressed in each of these tissues (Figure 2A, Figure S3A-D). We observed that in most cases *rde-4(-)* progeny were unable to silence the target gene upon feeding RNAi. The only exception was *unc-22* silencing in *rde-4(-)* progeny of parents expressing *rde-4(+)* under the body-wall muscle promoter *myo-3.* The extent of this silencing did not correlate with the rate of transmission of the extrachromosomal *Pmyo-3::rde-4(+)* array (Figure S3E) and silencing was also detected

in *rde-4(-)* progeny of animals with an integrated *Pmyo-3::rde-4(+)* array (Figure 2B). One explanation for this observation could be that the *myo-3* promoter is misexpressed at low levels within the germline and consequently, maternally deposited *rde-4* protein or mRNA enables silencing of *unc-22* when larvae are fed dsRNA. In sum, our results suggest that, with the possible exception of rescue using a *myo-3* promoter and silencing of *unc-22*, tissue-specific rescue of *rde-4* in somatic tissues of parents does not enable silencing of somatic genes in *rde-4(-)* progeny that ingest dsRNA. Therefore, cases of silencing in *rde-4(-)* tissues in response to tissue-specific expression of *rde-4(+)* (Figure 1) are likely due to the production of mobile RNA derivatives of ingested dsRNAs and not due to inheritance of parental RDE-4 protein by *rde-4(-)* tissues.

Silencing can occur in *rde-4(-)* cells when *rde-4* mosaic animals ingest dsRNA

Effects of mobile RNAs derived from ingested dsRNA can also be evaluated using mosaic analysis (Yochem and Herman 2003). In this approach, mosaic animals that result from the loss of rescuing DNA during mitosis are examined. Perdurance of protein or mRNA after the loss of rescuing DNA in ancestral cells can complicate the interpretation of effects in descendent cells, which is a different caveat compared to that for tissue-specific rescue. Therefore, to complement our analysis using tissue-specific rescue, we examined silencing by ingested dsRNA in *rde-4(-)* mosaic animals. Specifically, we co-expressed *rde-4(+)* and *DsRed* under the control of the *sur-5* promoter, which drives expression in all somatic cells, and examined silencing of *gfp* upon feeding RNAi of an integrated *Psur-5::sur-5::gfp* transgene in mosaic animals. This results in animals with an extrachromosomal array where cells that have the DNA for

rde-4(+) expression are marked with *DsRed* expression. In all 19 mosaic animals examined, silencing was observed in *rde-4(+)* as well as in *rde-4(-)* cells (Figure 3D). Taken together with the results from tissue-specific rescue of *rde-4*, these results are consistent with the hypothesis that some derivatives of ingested dsRNA generated in somatic tissues with *rde-4(+)* expression are transported between cells and are thus mobile.

Expression of a repetitive transgene in a tissue can inhibit silencing in that tissue

Intriguingly, we observed several cases of reduced silencing specifically within cells that express the *rde* gene in *rde* mosaic animals and in animals with tissue-specific rescue of *rde*. In *rde-4* mosaic animals, silencing was less efficient in cells that showed expression of *rde-4(+)* than in cells that lacked expression of *rde-4(+)* (e.g. the single binucleated intestinal cell in Figure 3D). In animals with tissue-specific rescue of *rde-4*, silencing of *gfp* (Figure 4A,B) or *unc-54* (Figure S4B) within body-wall muscles that express *rde-4(+)* and silencing of *bli-1* or *dpy-7* within hypodermal cells that express *rde-4(+)* (Figure S4C,D) were not detectable. In animals with tissue-specific rescue of *rde-1*, silencing of *gfp* (Figure S1B,C) or *unc-54* (Figure S4E) in body-wall muscles that express *rde-1(+)* was reduced.

To test if these cases of reduced silencing could be explained by insufficient levels of *rde* expression, we overexpressed *rde-4(+)* in the hypodermis of wild-type animals and measured silencing of *bli-1* and of *dpy-7* by ingested dsRNA (Figure 4C, second set of bars). Animals with the extrachromosomal *rde-4(+)* transgene failed to detectably silence *bli-1* or *dpy-7*. Thus, the observed lack of silencing is not because

there is insufficient *rde-4(+)* expression, but because expression of *rde-4(+)* within a tissue from a repetitive transgene inhibits feeding RNAi in that tissue. To test if the inhibition was because of high levels of *rde-4(+),* co-suppression (Napoli *et al*. 1999) of *rde-4*, or expression from a repetitive transgene, we expressed *gfp* from a repetitive transgene in the hypodermis and examined silencing of *bli-1* and of *dpy-7* by feeding RNAi. No silencing was detected in the presence of *gfp* expression (Figure 4C, fourth panel), suggesting that inhibition of silencing is the result of expression from a repetitive transgene and not because of *rde-4* expression or co-suppression. Similar reduction of silencing was also observed in body-wall muscles when we expressed *DsRed* from repetitive transgenes in body-wall muscles (Figure 4D-F). Consistently, tissue-specific expression of *rde-4(+)* in the hypodermis from a single-copy transgene enabled silencing of both *dpy-7* and *bli-1* by feeding RNAi (Figure 4G). This silencing was also inhibited by expression of *gfp* in the hypodermis from a repetitive transgene (Figure 4G). Thus, expression from a repetitive transgene and not high levels of *rde-4(+)* is the likely reason for the observed inhibition of feeding RNAi in *rde-4* mosaic animals and in animals with tissue-specific *rde-4* rescue.

Repetitive transgenes can produce dsRNA (Hellwig and Bass 2008) that might compete with ingested dsRNA for engaging the gene silencing machinery within a cell. Such competition between pathways has been proposed as the reason why enhanced silencing in response to feeding RNAi can occur in animals that lack genes required solely for the processing of endogenous dsRNA (Lee *et al.* 2006). During endogenous RNAi, the RdRP RRF-3 and the exonuclease ERI-1 produce dsRNA that is processed

by the endonuclease DCR-1 and the primary Argonaute ERGO-1 into guide RNAs, which are used to subsequently silence genes of complementary sequence (Figure 4H and reviewed in Billi *et al.* 2014). Loss of components required solely for the processing of endogenous dsRNA (*rrf-3*, *eri-1*, and *ergo-1*) has been shown to enhance feeding RNAi (Zhuang *et al.* 2011). Similar enhancement of silencing could potentially relieve the inhibition of feeding RNAi caused by expression from repetitive transgenes. We found that loss of *rrf-3* or of *eri-1* but not of *ergo-1* eliminated inhibition of feeding RNAi by expression from a repetitive transgene within the hypodermis (Figure 4I). Because RRF-3 and ERI-1 are not required for the production of dsRNA from repetitive transgenes (Kim *et al.* 2005), these results suggest that silencing by feeding RNAi in the presence of expression from a repetitive transgene is enabled by loss of dsRNA production at endogenous loci (see Figure S9 in Blumenfeld and Jose 2016).

Together, our results suggest that expression from some repetitive DNA in a tissue interferes with silencing by ingested dsRNA of some genes within that tissue.

Silencing in tissues that lack *rde-4* expression is observed only in animals with high levels of tissue-specific *rde-4* expression

Despite inhibition of silencing within tissues that express *rde-4(+)* from a repetitive transgene, robust silencing in tissues that lack *rde-4* was observed in animals with tissue-specific *rde-4* rescue and in *rde-4* mosaic animals (Figure 1, Figure 3, and Figure S2). To test if similar silencing in tissues that lack *rde-4* can occur when *rde-4(+)* is expressed within a tissue using a single-copy transgene, we subjected animals with tissue-specific *rde-4* rescue in the hypodermis to feeding RNAi against genes expressed

in the hypodermis (*bli-1*), the body-wall muscles (*unc-22*), or the intestine (*act-5*) and measured silencing. While silencing of *bli-1* was comparable to that in wild-type animals, silencing of *unc-22* or *act-5* was barely detectable (Figure 5, top). This lack of silencing in tissues that lack *rde-4* expression could either be because such silencing requires expression of any repetitive transgene within the *rde-4(+)* tissue or because it requires high levels of *rde-4(+)* expression. Two observations support the latter possibility: (1) silencing in tissues that lack *rde-4* was not detected even when hypodermal expression of *rde-4(+)* from the single-copy transgene was combined with hypodermal expression of *gfp* from a repetitive transgene (Figure 5, bottom); and (2) the level of *rde-4(+)* mRNA in animals with repetitive transgenes was higher than that of animals with the single-copy transgene (Figure S5). Together these results suggest that silencing by mobile RNAs derived from ingested dsRNA in tissues that lack *rde-4* requires the high levels of *rde-4(+)* expression within a tissue that can be achieved through expression from repetitive transgenes.

Site of *rde-4* expression dictates pattern of silencing in cells that lack *rde-4* expression

When an animal is only scored as silenced versus not silenced in response to feeding RNAi, qualitative differences between animals (e.g. silencing in different subsets of cells) are overlooked. Examination of such differences requires a target gene whose silencing in subsets of cells can be discerned in each animal. We found that null mutants of the hypodermal gene *bli-1* result in a fluid-filled sac (“blister”) along the entire worm (Figure S6A-C; Brenner 1974), and that blisters that form upon feeding RNAi in

wild-type animals had a different pattern (Figure 6A). Specifically, when the worm is divided into eight sections (Figure 6A, top), anterior sections tended to be more susceptible to silencing when compared with posterior sections, resulting in a stereotyped pattern of relative susceptibility to blister formation upon *bli-1* feeding RNAi (Figure 6A, bottom and Figure S6E). This bias in the tendency to form blisters could reflect the graded uptake of dsRNA from the anterior to the posterior in the intestine upon feeding RNAi. These characteristics of blister formation as a result of *bli-1* silencing enable examination of qualitative differences, if any, between silencing in wild-type animals and in animals with tissue-specific *rde-4* rescue.

Silencing of *bli-1* in animals with tissue-specific rescue of *rde-4* in non-hypodermal tissues was associated with variations in the stereotyped pattern of blister formation (Figure 6B-D). Specifically, *rde-4(-)* animals with high levels of *rde-4(+)* expression, assumed based on the high levels of *gfp* coexpressed from the same promoter, in posterior intestinal cells displayed a higher relative frequency of posterior blisters than did wild-type animals (Figure 6B and Figure S6F,G). To systematically analyze such differences, we culled animals that had a pattern of blister formation that differed from a reference blister susceptibility pattern observed in most wild-type animals (see methods). We found that unlike in wild-type animals, in animals with tissue-specific *rde-4* rescue, patterns of blisters that differed from the reference pattern were common (Figure 6C,D). Furthermore, the pattern of variant blister susceptibility differed depending on the tissue in which *rde-4(+)* was expressed (neurons vs. body-wall muscles) and not on the promoter used (*Prgef-1* or *Punc-119* for neurons and

Pmyo-3 or *Punc-54* for body-wall muscles) (Figure 6C,D and Figure S6H). Taken together, these results suggest that dsRNA-derived mobile RNAs generated by expression of *rde-4(+)* in different tissues cause different patterns of silencing in *rde-4(-)* tissues: mobile RNAs derived from ingested dsRNA appear to cause silencing in nearby *rde-4(-)* hypodermal cells.

Ingested dsRNA and their mobile RNA derivatives have different requirements for gene silencing

The ability to examine qualitative differences in silencing of *bli-1* provides an opportunity to determine differences, if any, between silencing by ingested dsRNA and silencing by dsRNA-derived mobile RNAs.

To determine the pathway through which silencing of *bli-1* occurs in response to ingested dsRNA, we examined silencing in animals that lack genes required for the canonical RNAi pathway (reviewed in Grishok 2013). We found that in addition to the dsRNA-binding protein RDE-4, the primary Argonaute RDE-1, and the RNA-dependent RNA polymerase RRF-1, genes that act in the nuclear RNAi pathway (the nuclear Argonaute NRDE-3 (Guang et al., 2008; Mao et al., 2015) and downstream components NRDE-2, NRDE-1, and NRDE-4) were also required for *bli-1* silencing in response to ingested dsRNA (Figure 7A).

To test if mobile RNAs derived from ingested dsRNA also require the nuclear RNAi pathway for silencing *bli-1*, we examined genetic requirements for blister formation upon *bli-1* feeding RNAi in animals with *rde-4* rescue in non-hypodermal tissues. While no silencing of *bli-1* was detected in the absence of *rde-1* or of *rrf-1* when *rde-4* was

rescued in neurons, substantial silencing could be detected in the absence of *nrde-3* when *rde-4* was rescued in neurons, in body-wall muscles, or in the intestine (Figure 7B,C and Figure S7A). Furthermore, the patterns of blister formation observed in the absence of *nrde-3* were different from those observed in the presence of *nrde-3* (compare Figure 7C with Figure 6D, also see Figure S7B). These results suggest that *bli-1* silencing by mobile RNAs derived from ingested dsRNA can occur independent of NRDE-3, potentially using one of the many other Argonautes in *C. elegans* (Yigit *et al.* 2006). Similar *nrde-3*-independent silencing of *bli-1* was also observed upon loss of *eri-1* or upon overexpression of *rde-4(+)* in hypodermal cells from a single-copy transgene (Figure S7C-E). However, expression of *bli-1* dsRNA in neurons resulted in *bli-1* silencing that depended on both *sid-1* and *nrde-3* (Figure 7D), suggesting that mobile RNAs derived from ingested dsRNA and mobile RNAs made from neuronal dsRNA have different requirements for silencing *bli-1*. Thus, unlike silencing by ingested dsRNAs and neuronal mobile RNAs, silencing by mobile RNAs derived from ingested dsRNA is akin to silencing in an enhanced RNAi background or silencing within a tissue with RDE-4 overexpression and can occur independent of the nuclear RNAi pathway.

Because silencing by ingested dsRNA and by ingested dsRNA-derived mobile RNAs appear to have different requirements, we wondered if silencing by both forms of dsRNA were equally susceptible to inhibition by expressed repetitive transgenes. To test for inhibition, we expressed *gfp* from a repetitive transgene in the hypodermis of wild-type animals or *rde-4(-)* animals with *rde-4(+)* in body-wall muscles and examined silencing in response to feeding RNAi of the hypodermal genes *dpy-7* or *bli-1*. Unlike

silencing by ingested dsRNA, silencing by their mobile RNA derivatives was not robustly inhibited (Figure 7E).

In summary, our results suggest that silencing of a gene by ingested dsRNA-derived mobile RNAs has different requirements compared to those for silencing of the same gene by ingested dsRNA or by neuronal mobile RNAs (Figure 8A).

DISCUSSION

Our analyses of feeding RNAi in *C. elegans* reveal that high levels of RDE-4 in one somatic tissue can generate dsRNA-derived mobile RNAs that can silence a gene in other somatic tissues but not in the germline (Figure 8B). Silencing by ingested dsRNA and by dsRNA-derived mobile RNA can be distinguished based on their differential requirement for the nuclear Argonaute NRDE-3 to silence the hypodermal gene *bli-1* and their differential susceptibility to inhibition by expression from repetitive DNA (Figure 8A).

Mobile RNAs derived from ingested dsRNAs could be chemically modified short dsRNAs

Ingested dsRNA can be transported across the intestine and accumulate in the fluid-filled body cavity without entry into the cytosol of intestinal cells in *C. elegans* (Jose *et al.* 2009; Calixto *et al.* 2010; Hinas *et al.* 2012). Additionally, dsRNA-derived mobile RNAs made from multiple tissues (intestine, body-wall muscles, hypodermis, and neurons in Figure 1) can be present in the body cavity. Our results reveal three differences between silencing by these two forms of extracellular dsRNA – differential silencing of germline genes, differential requirements for a nuclear Argonaute, and differential susceptibility to inhibition by repetitive transgenes. One explanation for these differences could be quantitative differences in the amounts of ingested dsRNAs and their mobile RNA derivatives delivered into the target tissues. Alternatively, we speculate that cells could distinguish ingested dsRNA from their mobile RNA derivatives.

Three considerations suggest that mobile RNAs derived from ingested dsRNA are chemically modified short dsRNAs. First, the requirement for processing by RDE-4 but not by RDE-1 to generate dsRNA-derived mobile RNAs (Figure 1) suggests that they are short dsRNAs. Second, the inability of dsRNA-derived mobile RNAs to cause silencing within the germline (Figure 1) is consistent with them being short dsRNAs because RNAs need to be longer than 50 bp for entry into the germline and/or for subsequent silencing (Feinberg and Hunter 2003). Third, terminal chemical modification of dsRNA-derived mobile RNAs could be the basis for the ability of these RNAs to bypass the requirement for the Argonaute NRDE-3 (Figure 7B&C) because Argonautes recognize small RNAs by binding to their termini (Czech *et al*. 2011) and because the putative nucleotidyltransferase MUT-2 is also required for the generation of mobile RNAs from ingested dsRNAs (Jose *et al*. 2011).

Efficiency of RNAi could be regulated by expression from repetitive DNA

Our discovery that expression from repetitive DNA within a tissue can interfere with silencing by feeding RNAi within that tissue (Figure 4) raises concerns for the use of RNAi to infer the function of a gene. For example, RNAi of a gene in strains that express fluorescent reporters within a tissue from a repetitive transgene could be specifically inhibited in that tissue resulting in differences between the defects observed upon RNAi of a gene and those observed upon mutation of that gene. Thus, inferences from past experiments that used feeding RNAi in the presence of tissue-specific expression from repetitive transgenes may need to be revised.

The efficiency of feeding RNAi differs in different tissues and is a key concern for the application of feeding RNAi to combat animal pests (Koch and Kogel 2014). For example, in *C. elegans*, genes expressed in neurons are relatively refractory to silencing by feeding RNAi (noted in Tavernarakis *et al.* 2000). One reason for such reduced silencing could be that neurons have high levels of expression from endogenous repetitive DNA. Consistent with this possibility, both silencing in tissues with expression from repetitive DNA (Figure 4I) and silencing in neurons are enhanced upon loss of the exonuclease ERI-1 (Kennedy *et al.* 2004) or the RdRP RRF-3 (Simmer *et al.* 2002). Thus, when feeding RNAi is used against animal pests, expression from endogenous repetitive DNA could cause resistance to silencing.

Ingested dsRNA could engage similar mechanisms in many invertebrates

Feeding RNAi can be used to silence essential genes in many insects and parasitic nematodes (see Jose 2015; Koch and Kogel 2014; Lilley *et al.* 2012 for reviews). Recent studies suggest that several characteristics of feeding RNAi in these invertebrates are similar to those in *C. elegans*. First, long dsRNA (>60 bp) is preferentially ingested (Bolognesi *et al.* 2012) and realization of this preference was crucial for developing plastid expression as an effective strategy to deliver long dsRNA into crop pests (Zhang *et al.* 2015). Second, dsRNA can be detected in intestinal cells and in internal tissues upon feeding RNAi (Ivashuta *et al.* 2015). Third, with the exception of dipteran insects, most invertebrates have homologs of the dsRNA importer SID-1 (Tomoyasu *et al.* 2008). Finally, silencing initiated by feeding RNAi can persist for multiple generations (Abdellatef *et al.* 2015). These similarities suggest that insights

gleaned using the tractable animal model *C. elegans* are likely to be applicable to many invertebrates - including agronomically important insect and nematode pests.

ACKNOWLEDGEMENTS

We thank Leslie Pick and members of the Jose lab for critical reading of the manuscript; Julia Marre (Jose lab) for generating the plasmid pJM6; Yun Choi (Jose lab) for generating the plasmid pYC13; the *Caenorhabditis elegans* Genetic stock Center, the Hunter lab (Harvard University), and the Seydoux lab (Johns Hopkins University) for some worm strains and the Hamza lab (University of Maryland) for bacteria that express *gfp-dsRNA*. Critical comments from anonymous reviewers were crucial in arriving at the working model proposed in this manuscript. This work was supported in part by National Institutes of Health Grant R01GM111457 (to A.M.J.)

FIGURES AND FIGURE LEGENDS

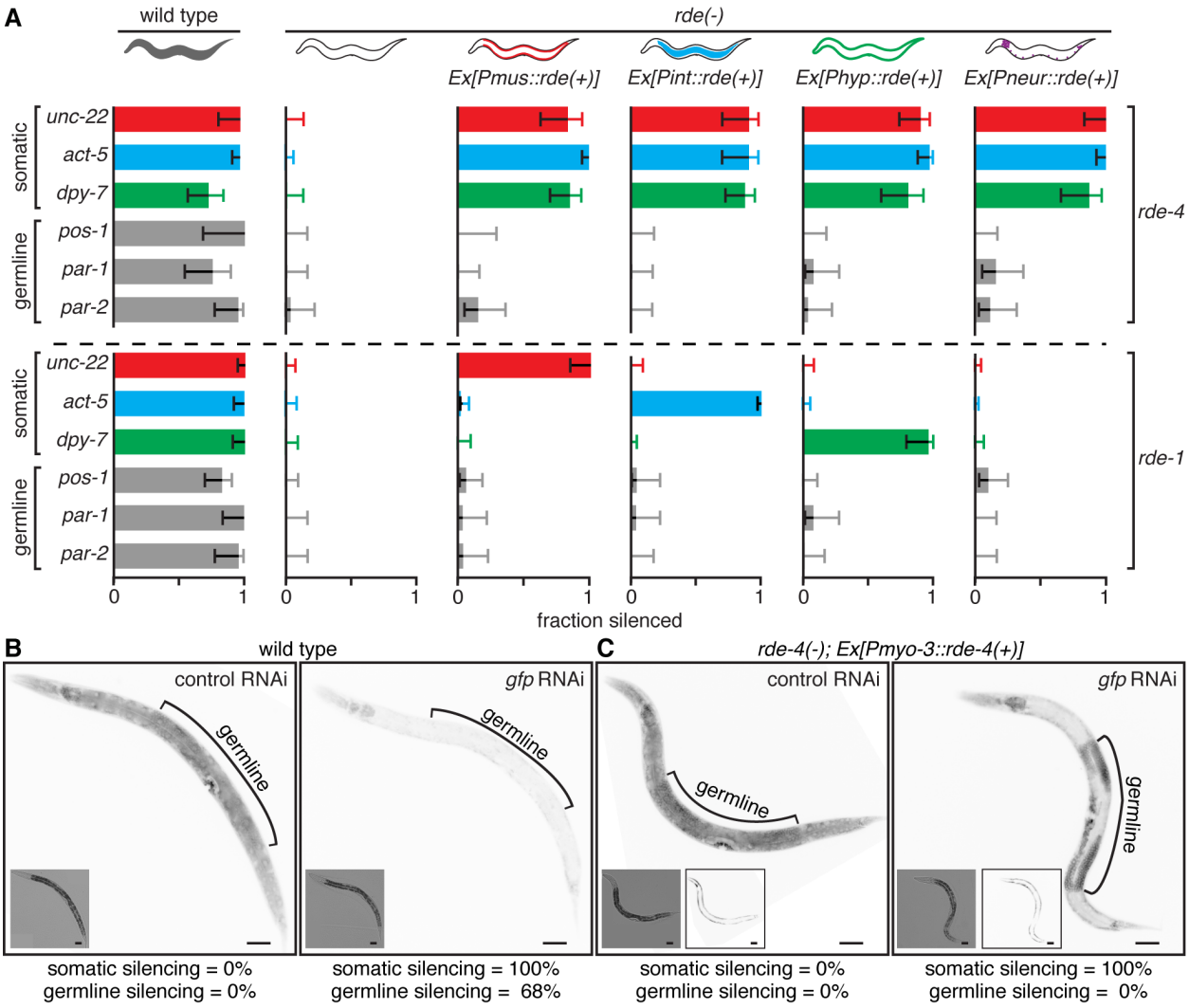

Figure 1 Expression of RDE-4 in a tissue enables silencing in somatic tissues that lack *rde-4* expression but not in the germline that lacks *rde-4* expression. (A) Tissue-specific expression of RDE-4 but not RDE-1 enables silencing of genes that function in mutant somatic tissues but not in mutant germline. Wild-type animals (grey), mutant animals (*rde-4(-)* or *rde-1(-)*, white), and mutant animals with tissue-specific rescues of *rde-1* or *rde-4* (colors within worms) were fed dsRNA against genes expressed in somatic tissues (the body-wall muscle (*unc-22*, red), intestine (*act-5*, blue), hypodermis (*dpy-7*,

green)), or in the germline (*pos-1*, *par-1* or *par-2*, grey) and the fractions of animals that showed silencing (fraction silenced) were determined. Wild-type genes (*rde-4* or *rde-1*) were expressed in the body-wall muscles using *Pmyo-3* (*Ex[Pmus::rde(+)],* red), in the intestine using *Psid-2* (*Ex[Pint::rde(+)]*, blue), in the hypodermis using *Pwrt-2* (*Ex[Phyp::rde(+)]*, green), or in neurons using *Prgef-1* (*Ex[Pneur::rde(+)]*, purple). Error bars indicate 95% CI and n>24 animals. (B and C) Tissue-specific rescue of *rde-4* enables silencing of *gfp* in *rde-4(-)* somatic tissue but not in *rde-4(-)* germline. Representative images of animals with *gfp* expression in all somatic and germline cells (*Pgtbp-1::gtbp-1::gfp*) in a wild-type background (B), or *rde-4(-)* background with *rde-4(+)* expressed in body-wall muscles (C, *Ex[Pmyo-3::rde-4(+)*) that were fed either bacteria with no dsRNA (control RNAi, *left*) or bacteria that express dsRNA against *gfp* (*gfp* RNAi, *right*) are shown. Percentages of animals showing silencing in somatic cells and germline are indicated. Insets are brightfield images and scale bar = 50 μm, n=50. Also see Figure S2.

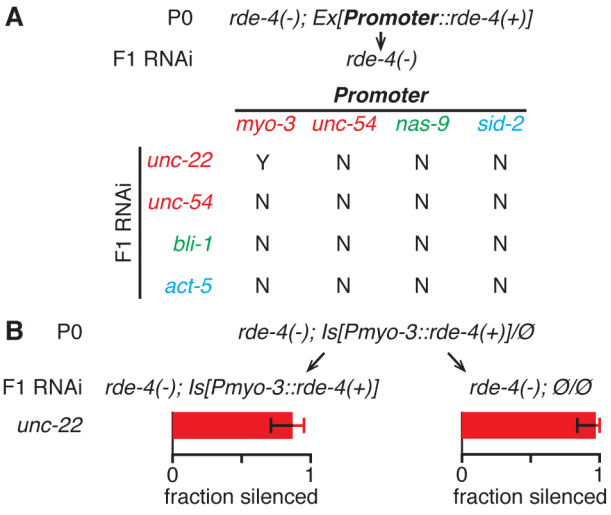

Figure 2 Expression of RDE-4 in the somatic tissues of parents does not typically enable feeding RNAi in *rde-4(-)* progeny. (A) Parental expression of *rde-4(+)* enables feeding RNAi in *rde-4(-)* progeny only in the case of *unc-22* silencing with *Pmyo-3* driven *rde-4* expression among 16 promoter/gene combinations tested. The *rde-4(-)* progeny of parents with *rde-4* rescued using tissue-specific promoters (body-wall muscle (*myo-3* or *unc-54*, red), hypodermis (*nas-9*, green), or intestine (*sid-2*, blue)) were subjected to feeding RNAi (F1 RNAi) of genes in the body-wall muscle (*unc-22* and *unc-54*, red), hypodermis (*bli-1*, green), or intestine (*act-5*, blue) and scored for silencing (Y = yes; N = no). See Figure S3A-D for quantification of each feeding RNAi. (B) Parental expression of *rde-4(+)* from an integrated *Pmyo-3::rde-4(+)* transgene also enables feeding RNAi of *unc-22* in *rde-4(-)* progeny. The *rde-4(+)* progeny (*Is[Pmyo-3::rde-4(+)*]) and *rde-4(-)* progeny (*Ø/Ø*) of parent animals expressing RDE-4 from an integrated array were subjected to feeding RNAi (F1 RNAi) of *unc-22* and the fraction of animals that showed silencing were determined (fraction silenced). 100% of wild-type and 0% of *rde-4(-)* control animals showed silencing of *unc-22*. Also see Figure S3E. Error bars indicate 95% CI and n>20 animals.

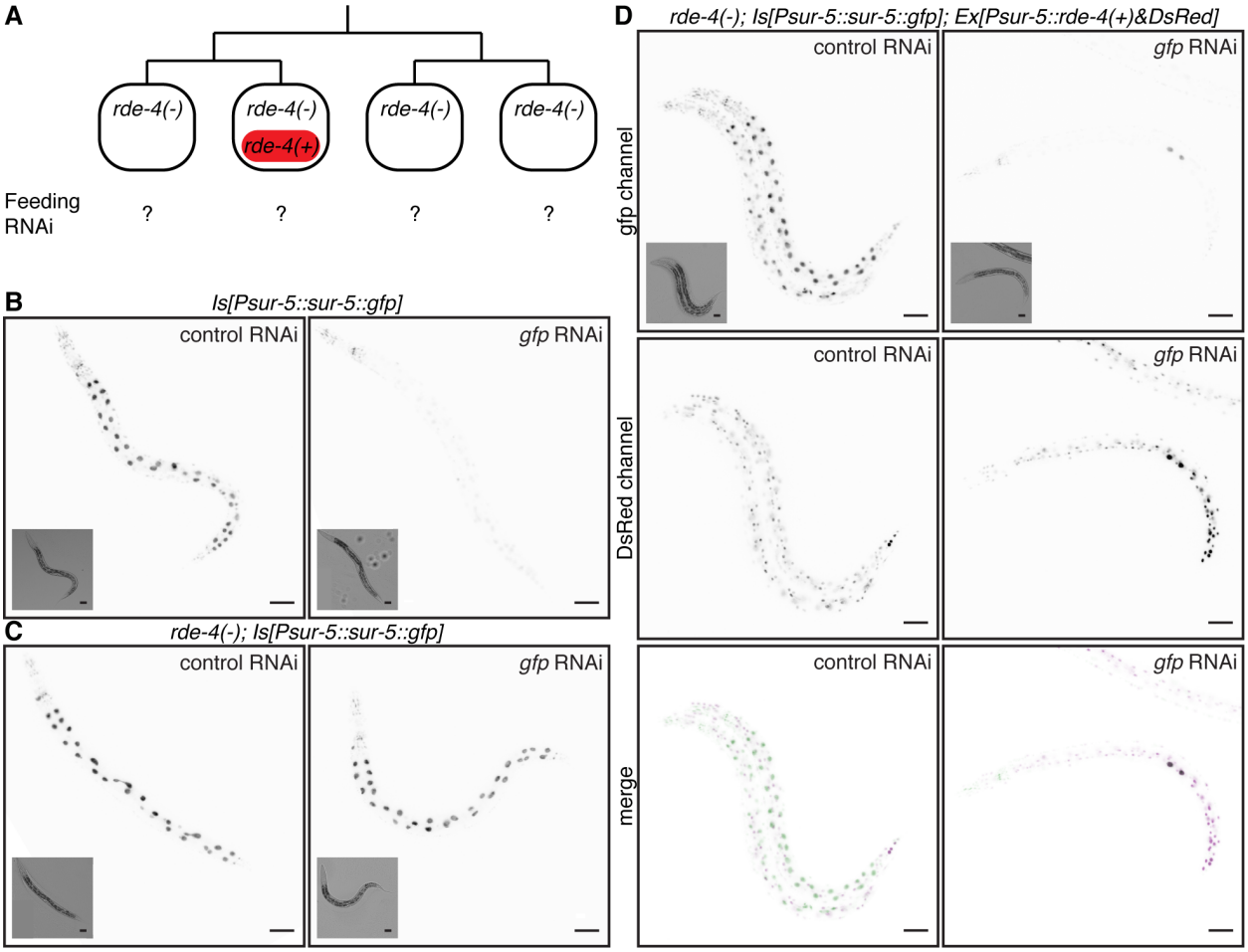

Figure 3 *rde-4(-)* cells can be silenced by ingested RNAi in *rde-4* mosaic animals. (A) Schematic of *rde-4* mosaic analysis. Animals with mitotic loss of rescuing DNA resulting in some mutant cells (*rde-4(-)*) and some wild-type cells (*rde-4(+)* with co-expressed *DsRed*) were fed dsRNA targeting a gene expressed in both mutant cells and wild-type cells and the resultant silencing (feeding RNAi - ?) was examined. (B to D) Representative images of animals with *gfp* expression in all somatic nuclei (*Is[Psur-5::sur-5::gfp]*) in wild-type animals (B), *rde-4(-)* animals (C) or *rde-4* mosaic animals with *rde-4* rescue marked with *DsRed* expression (*Ex[Psur-5::rde-4(+)&DsRed]*) (D) that were fed control dsRNA (control RNAi, left) or dsRNA against *gfp* (*gfp* RNAi, right) are shown (n > 9 in (B) and n > 10 in (C); and n>12 in (D)). Merged images in (D) show

overlap of *gfp* and *DsRed* expression (red channel = magenta; green channel = green; and merge = black). Insets are brightfield images and scale bar = 50μm.

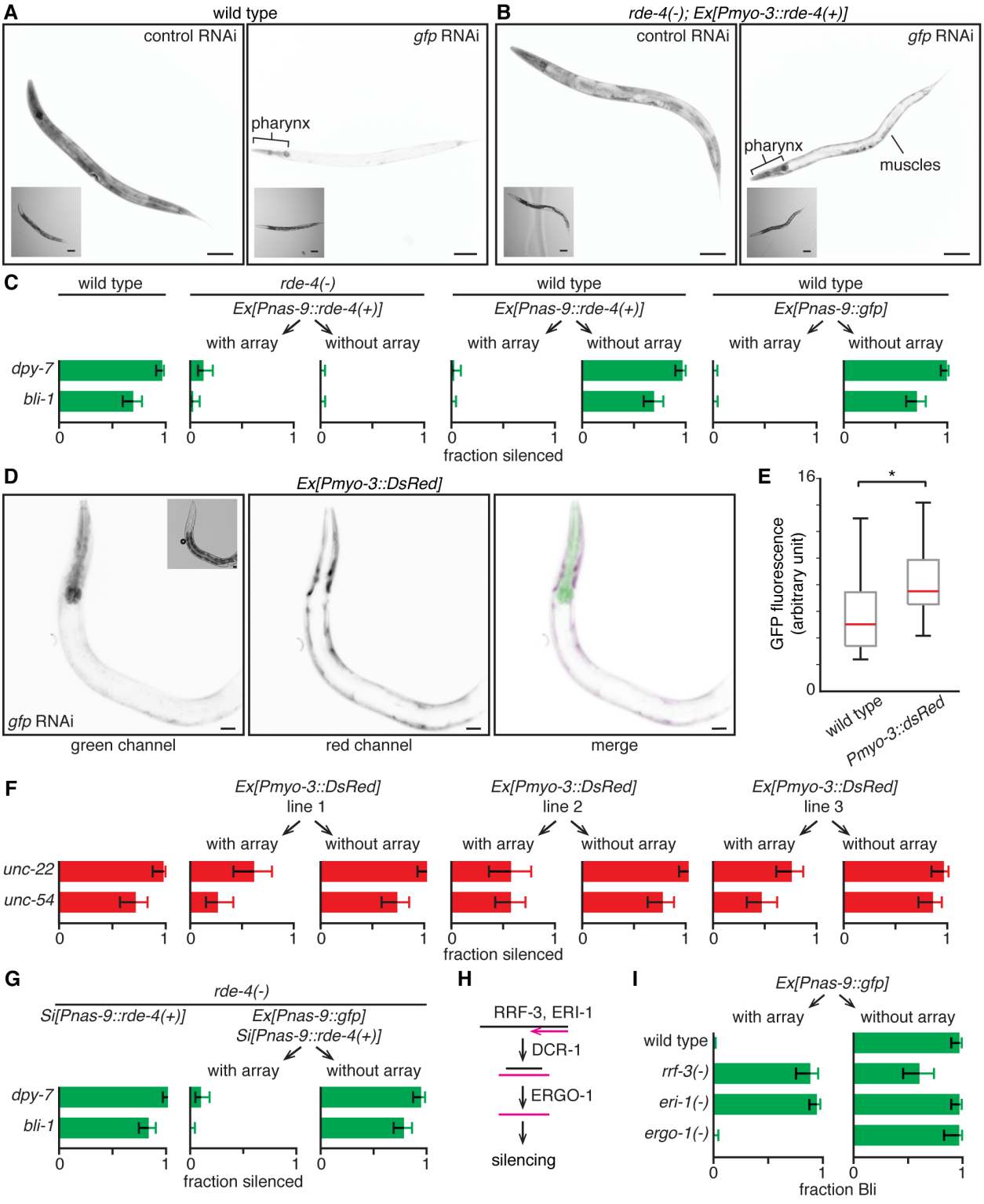

Figure 4 In the presence of some components of endogenous RNAi, expression of repetitive DNA within a tissue can inhibit feeding RNAi within that tissue. (A and B) Silencing of a gene in body-wall muscles that express *rde-4(+)* from a repetitive transgene is reduced despite potent silencing of the same gene in *rde-4(-)* tissues. Representative images of animals with *gfp* expression in all somatic cells (*Peft-3::gfp*) in a wild-type background (A) or *rde-4(-)* background with *rde-4(+)* expressed in body-wall muscles (*Ex[Pmyo-3::rde-4(+)*) (B) that were fed either bacteria with no dsRNA (control RNAi, *left*) or bacteria that express dsRNA against *gfp* (*gfp* RNAi, *right*) are shown. Tissues that show reduced silencing (pharynx, muscles) are labeled, insets are brightfield images and scale bar = 50 μm. Also see Figure S1 and Figure S4A. (C) Silencing of *bli-1* and *dpy-7* is inhibited by the expression of a repetitive transgene of unrelated sequence in the hypodermis. Wild-type animals and *rde-4(-)* animals that express *rde-4(+)* along with *gfp* in the hypodermis (*Ex[Pnas-9::rde-4(+)]*) from extrachromosomal repetitive DNA (array) or wild-type animals that express *gfp* alone in the hypodermis (*Ex[Pnas-9::gfp]*) from extrachromosomal repetitive DNA (array) were fed dsRNA against hypodermal genes (*dpy-7* or *bli-1*, green). The fractions of animals either with or without the arrays that showed silencing (fraction silenced) were determined. (D and E) Silencing of *gfp* in body-wall muscles that express *DsRed* from a repetitive transgene, upon feeding RNAi, is reduced despite potent silencing of *gfp* in other tissues. (D) Representative images of animal expressing *DsRed* in the body-wall muscles (*Ex[Pmyo-3::DsRed],* red channel) with *gfp* expression in all somatic cells (green channel) that were fed bacteria that express dsRNA against *gfp* (*gfp* RNAi) are

shown. Merged images show overlap of *gfp* and *DsRed* expression (red channel = magenta; green channel = green; and merge = black). Insets are brightfield images and scale bar = 50 μm. Also see Figure S4F,G. (E) Quantification of *gfp* silencing in animals with or without *DsRed* expression in body-wall muscles. In animals expressing *DsRed* in the body-wall muscles (*Ex[Pmyo-3::DsRed]*) expression of *gfp* was observed to be prominent in the body-wall muscles. Red lines indicates median GFP fluoresence. Asterisk indicates P<0.05, Student's t-test. (F) Silencing of *unc-22* and *unc-54* can be inhibited by the expression of a repetitive transgene of unrelated sequence in body-wall muscles. Three lines of wild-type animals expressing *DsRed* in the body-wall muscle (*Ex[Pmyo-3::DsRed]*) from extrachromosomal repetitive DNA (array) were fed dsRNA against body-wall muscle genes (*unc-22* or *unc-54*, red). The fractions of animals either with or without the arrays that showed silencing (fraction silenced) were determined. Silencing in all lines were significantly inhibited compared to wild type animals (p<0.01) except silencing of *unc-54* in line 2 (G) Expression of *rde-4(+)* from a single-copy transgene within a tissue does not inhibit feeding RNAi of a gene in that tissue. *rde-4(-)* animals that express *rde-4(+)* in the hypodermis from a single-copy transgene (*Si[Pnas-9::rde-4(+)]*) or that additionally express *gfp* in the hypodermis (*Ex[Pnas-9::gfp]*) from a repetitive transgene (array) were fed dsRNA against *dpy-7* or *bli-1* and animals with or without the *gfp* array were analyzed as in C. (H and I) Inhibition of *bli-1* silencing by expression of any repetitive DNA can be relieved by the loss of some components of the endogenous RNAi pathway. (H) Schematic of endogenous RNAi. Aberrant RNA recruits the RNA-dependent RNA polymerase RRF-3, the exonuclease ERI-1, the endonuclease

DCR-1, and the primary Argonaute ERGO-1 to cause silencing. (I) Loss of *eri-1* or *rrf-3* but not of *ergo-1* relieves inhibition of *bli-1* silencing caused by hypodermal expression of repetitive DNA. Extent of silencing (fraction Bli) in response to *bli-1* feeding RNAi of animals with or without an extrachromosomal array that expresses *gfp* in the hypodermis (*Ex[Pnas-9::gfp]*) in a wild-type, *rrf-3(-)*, *eri-1(-)*, or *ergo-1(-)* background were determined. Error bars indicate 95% confidence intervals and n>18 animals.

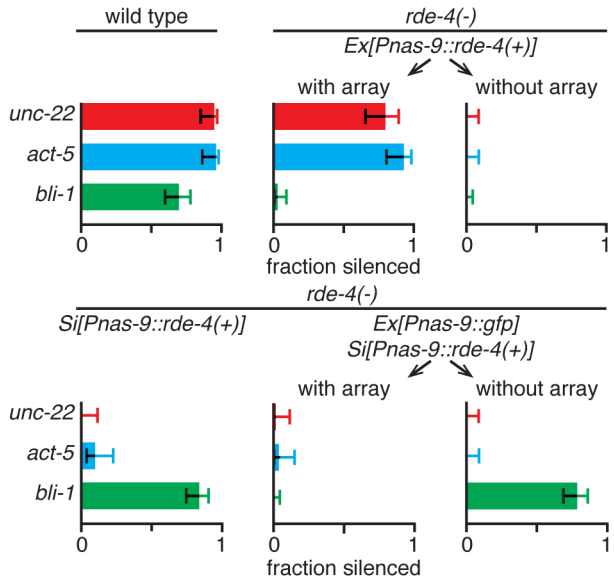

Figure 5 Silencing in a somatic tissue that lacks *rde-4* expression likely requires high levels of *rde-4(+)* in another tissue. *rde-4(-)* animals that express *rde-4(+)* from a repetitive transgene in the hypodermis (*Ex[Pnas-9::rde-4(+)]*) or from a single-copy transgene in the hypodermis (*Si[Pnas-9::rde-4(+)]*) or *gfp* from a repetitive transgene (*Ex[Pnas-9::gfp]*) in addition to *Si[Pnas-9::rde-4(+)]*) were fed dsRNA against *unc-22* (red), *act-5* (blue) or *bli-1* (green). Silencing was scored as in Figure 1. Error bars indicate 95% CI and n>49 animals.

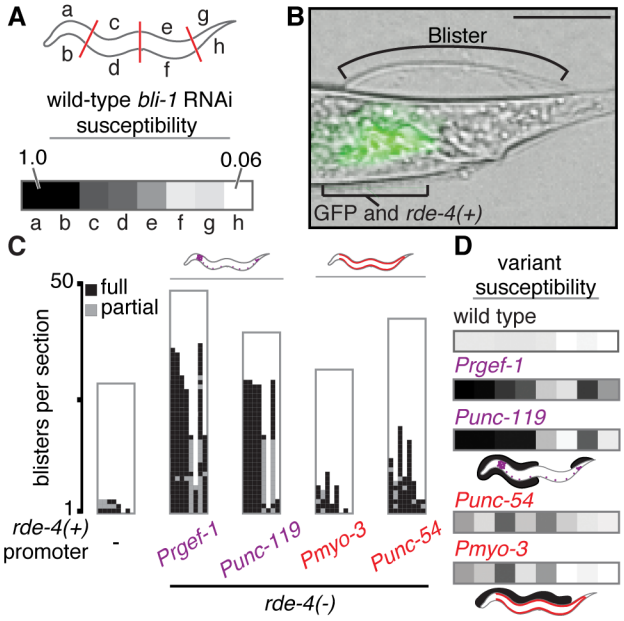

Figure 6 The pattern of blisters that results from silencing of *bli-1* in *rde-4(-)* hypodermis depends on the tissue that expresses RDE-4. (A) Susceptibility to *bli-1* feeding RNAi decreases from anterior to posterior hypodermis in wild-type animals. (top) Schematic of hypodermal sections (a through h) scored for blister formation. (bottom) Relative frequency of blister formation in each hypodermal section of wild-type animals upon *bli-1* feeding RNAi. The frequency ranged from 1.0 (black, a) to 0.06 (~white, h). (B) Frequency of blisters in *rde-4(-)* hypodermal cells near the tail correlate with levels of *rde-4(+)* expression in intestinal cells near the tail. Blisters were frequent near the tail upon *bli-1* feeding RNAi in animals with high (76% Bli, n=71) or low (48% Bli, n=28) *gfp* (and thus presumably *rde-4(+)*) expression but were rare in wild-type (10% Bli, n=300) animals. A representative animal with high *rde-4(+)* expression (inferred from high *gfp* expression) in tail intestinal cells with blister formation in nearby hypodermal cells is shown. (C and D) The pattern of blisters that result from silencing of *bli-1* in *rde-4(-)* hypodermis are characteristic of the tissue that expresses *rde-4(+)*. (C) Patterns of

blister formation in response to ingested *bli-1* RNAi were examined in wild-type animals or in *rde-4(-)* animals that express *rde-4(+)* under neuronal promoters (*Prgef-1* or *Punc-119,* purple) or under body-wall muscle promoters (*Pmyo-3* or *Punc-54*, red). For each strain, sections with full (black) or partial (grey) blister formation in animals that showed a variation in the order of susceptibility (i.e. were not a > b > … > h) were plotted. Grey bounding box indicates the total number of worms that showed blister formation in each strain (n = 50 gravid adult animals). (D) Aggregate patterns of blister formation among animals that deviate from the susceptibility order (variant susceptibility) for each section and for each strain. All strains being compared were normalized together (black, section with highest frequency of blisters in all strains; white, section with the lowest frequency of blisters in all strains). Schematic of worms indicate locations of variant blisters (thick black lines) on worms with *rde-4(+)* expressed in neurons (purple) or in body-wall muscles (red). Also see Figure S6.

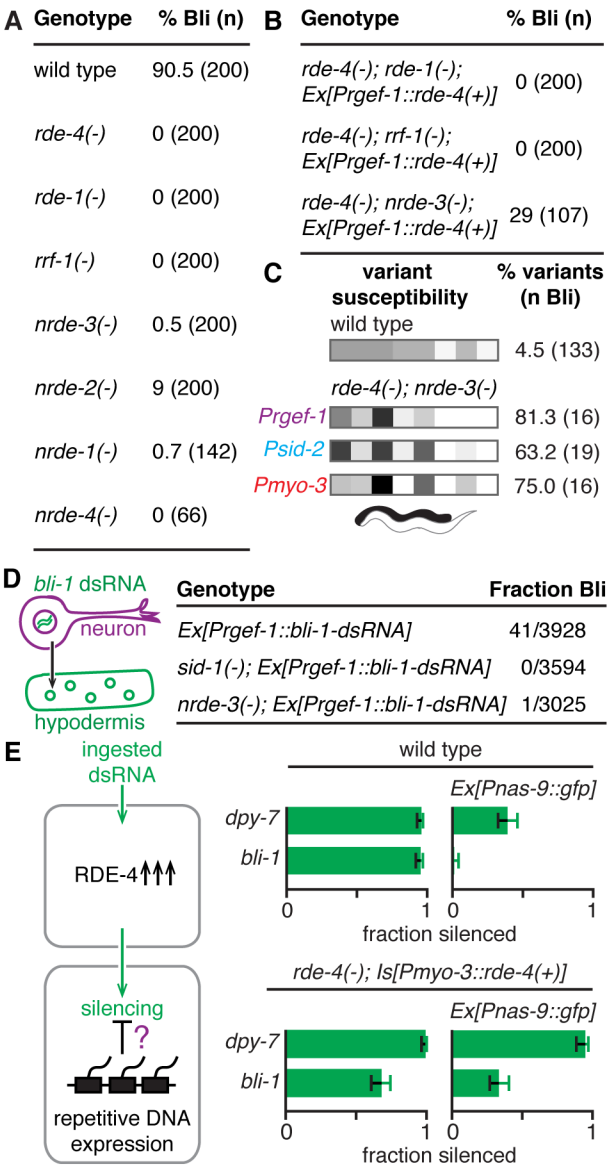

Figure 7 Silencing by mobile RNAs derived from ingested dsRNA, unlike silencing by ingested dsRNA or by neuronal mobile RNAs, can bypass the requirement for NRDE-3 and inhibition by expression from repetitive DNA. (A) Silencing of the hypodermal gene, *bli-1*, by ingested dsRNA requires the nuclear RNAi pathway. Wild-type, *rde-4(-)*, *rde-1(-)*, *rrf-1(-)*, *nrde-3(-)*, *nrde-2(-)*, *nrde-1(-)* or *nrde-4(-)* animals were fed dsRNA against *bli-1* and the percentage of animals that showed silencing (% Bli) were determined (n indicates number of gravid adults scored for silencing). (B) Mobile RNA derived from

ingested dsRNA targeting *bli-1* can bypass the requirement for the nuclear Argonaute NRDE-3. Double mutant animals that lack *rde-4* and either *rde-1*, *rrf-1*, or *nrde-3* but that each in addition express *rde-4(+)* under the control of a neuronal promoter (*Ex[Prgef-1::rde-4(+)]*) were analyzed as in A. (C) Patterns of blisters upon silencing *bli-1* in *nrde-3(-)* animals differs from that in wild-type animals but are similar across *rde-4(-)* animals that express *rde-4(+)* in multiple tissues. Aggregate patterns of variation in blister formation in wild type animals and *nrde-3(-); rde-4(-)* animals that express *rde-4(+)* in neurons (*Prgef-1*, purple), intestine (*Psid-2*, blue), or body-wall muscles (*Pmyo-3*, red) upon *bli-1* RNAi were determined as in Figure 6D. The percentage of animals with blister patterns that deviated from the consensus pattern (% variants) and the number of gravid adult animals among 150 analyzed gravid adult animals that show blister formation (n Bli) is indicated for each strain. (D) Silencing of *bli-1* by neuronal dsRNA requires the nuclear RNAi pathway. Silencing of *bli-1* by dsRNA against *bli-1* expressed under a neuronal promoter (*Ex[Prgef-1::bli-1-dsRNA]*) in a wild-type, *sid-1(-)* or *nrde-3(-)* background was measured as the fraction of gravid adult animals that showed blister formation (Fraction Bli) (Left, schematic of experiment; Right, data). (E) Silencing within tissues that lack *rde-4* expression in animals with tissue-specific rescue of *rde-4* is not inhibited by expression from repetitive DNA. Wild-type animals or *rde-4(-); Is[Pmyo-3::rde-4(+)]*) animals, both with or without *gfp* in the hypodermis (*Ex[Pnas-9::gfp]*), were fed dsRNA against *dpy-7* or *bli-1* (Left, schematic of experiment; Right, data). Silencing was scored as in Figure 1. Error bars indicate 95% CI and n>91. Also see Figure S7.

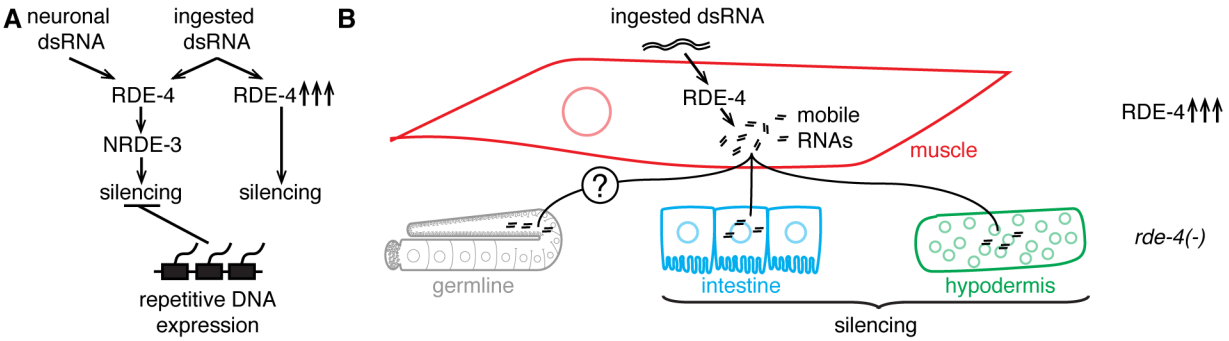

Figure 8 Working models for RNA processing and silencing upon feeding RNAi in *C. elegans* at an organismal level. Overexpression of RDE-4 within a somatic tissue generates mobile RNA derivatives of ingested dsRNAs, which have different requirements for silencing compared to ingested dsRNAs or neuronal mobile RNAs. (A) Silencing by mobile RNA derivatives of ingested dsRNAs can bypass requirements for the nuclear Argonaute NRDE-3 for *bli-1* silencing and inhibition by expression from repetitive DNA within a target tissue. (B) Silencing by mobile RNA derivatives of ingested dsRNAs made in one somatic tissue (e.g. body-wall muscles) can cause *rde-4*-independent silencing in other somatic tissues (e.g. intestine, hypodermis) but not within the germline – either reflecting the inability of the germline to import these RNAs (question mark) or the inability of the germline to use these RNAs for silencing.

REFERENCES

Abdellatef, E., T. Will, A. Koch, J. Imani, A. Vilcinskas, and K. H. Kogel, 2015 Silencing the expression of the salivary sheath protein causes transgenerational feeding suppression in the aphid Sitobion avenae. Plant Biotechnol. J. 13: 849-857.

Arribere, J. A., R. T. Bell, B. X. Fu, K. L. Artiles, P. S. Hartman, *et al.*, 2014 Efficient marker-free recovery of custom genetic modifications with CRISPR/Cas9 in *Caenorhabditis elegans*. Genetics 198: 837-846.

Baum, J. A., T. Bogaert, W. Clinton, G. R. Heck, P. Feldmann, *et al.*, 2007 Control of coleopteran insect pests through RNA interference. Nat. Biotechnol. 25: 1322–1326.

Billi, A. C., S. E. J. Fisher, and J. K. Kim, Endogenous RNAi pathways in *C.elegans*. WormBook, ed. *The C. elegans Research Community*, http://www.wormbook.org; 2014.

Blanchard, D., P. Parameswaran, J. Lopez-Molina, J. Gent, J. F. Saynuk, *et al.*, 2011 On the nature of in vivo requirements for *rde-4* in RNAi and developmental pathways in *C. elegans*. RNA Biol. 8: 458-467.

Blumenfeld, A., and A.M. Jose, 2016 Reproducible features of small RNAs in *C. elegans* reveal NU RNAs and provide insights into 22G RNAs and 26G RNAs. RNA 22:184–192.

Bolognesi, R., P. Ramaseshadri, J. Anderson, P. Bachman, W.Clinton, *et al.*, 2012 Characterizing the mechanism of action of double-stranded RNA activity against western corn rootworm (Diabrotica virgifera virgifera LeConte). PLoS One 7: e47534.

Brenner, S., 1974 The genetics of *Caenorhabditis elegans*. Genetics 77: 71–94.

Calixto, A., D. Chelur, I. Topalidou, X. Chen, and M. Chalfie, 2010 Enhanced neuronal RNAi in C. elegans using SID-1. Nat. Methods. 7: 554–559.

Czech, B., and G. J. Hannon, 2011 Small RNA sorting: matchmaking for Argonautes. Nat. Rev. Genet. 12: 19-31.

Devanapally, S., S. Ravikumar, and A. M. Jose, 2015 Double-stranded RNA made in *C. elegans* neurons can enter the germline and cause transgenerational gene silencing. Proc. Natl. Acad. Sci. USA. 112: 2133-2138.

Feinberg, E. H., and C. P. Hunter, 2003 Transport of dsRNA into cells by the transmembrane protein SID-1. *Science* **301**: 1545–1547.

Grishok, A., 2013 Biology and mechanisms of short RNAs in *Caenorhabditis elegans*. Adv. Genetics 83: 1-69.

Guang, S., A. F. Bochner, D. M. Pavelec, K. B. Burkhart, S. Harding, *et al.*, 2008 An Argonaute transports siRNAs from the cytoplasm to the nucleus. Science 321: 537–541.

Harfe, B. D., and A. Fire, 1998 Muscle and nerve-specific regulation of a novel NK-2 class homeodomain factor in *Caenorhabditis elegans*. Development 125: 421-429.

Hellwig, S., and B. L. Bass, 2008 A starvation-induced noncoding RNA modulates expression of Dicer-regulated genes. Proc. Natl. Acad. Sci. USA. 105: 12897–12902.

Hinas, A., A. J. Wright, and C. P. Hunter, 2012 SID-5 is an endosome-associated protein required for efficient systemic RNAi in *C. elegans*. Curr. Biol. 22: 1938-43.

Ivashuta, S., Y. Zhang, B. E. Wiggins, P. Ramaseshadri, G. C. Segers, *et al.,* 2015 Environmental RNAi in herbivorous insects. RNA 21: 840-850.

Jose, A. M. 2015 Movement of regulatory RNA between animal cells. Genesis 53: 395-416.

Jose, A. M., G. A. Garcia, and C. P. Hunter, 2011 Two classes of silencing RNAs move between *C. elegans* tissues. Nat. Struct. Mol. Biol. 18: 1184-1188.

Jose, A. M., J. J. Smith, and C. P. Hunter, 2009 Export of RNA silencing from *C. elegans* tissues does not require the RNA channel SID-1. Proc. Natl. Acad. Sci. USA. 106: 2283–2288.

Kamath, R. S., A. G. Fraser, Y. Dong, G. Poulin, R. Durbin, *et al*., 2003 Systemic functional analysis of the *Caenorhabditis elegans* genome using RNAi. Nature 421: 231-237.

Kennedy, S., D. Wang, and G. Ruvkun, 2004 A conserved siRNA-degrading RNase negatively regulates RNA interference in *C. elegans*. Nature 427: 645-649.

Kim, J. K., H. W. Gabel, R. S. Kamath, M. Tewari, A. Pasquinelli, *et al*., 2005 Functional genomic analysis of RNA interference in *C. elegans*. Science 208: 1164–1167.

Koch, A., and K. H. Kogel, 2014 New wind in the sails: improving the agronomic value of crop plants through RNAi-mediated gene silencing. Plant Biotechnol. J. 12: 821-831.

Lee, R., M. H. Christopher, and A. Ambros, 2006 Interacting endogenous and exogenous RNAi pathways in *Caenorhabditis elegans*. RNA 12: 589–597.

Lilley, C. J., L. J. Davies, and P. E. Urwin, 2012 RNA interference in plant parasitic nematodes: a summary of the current status. Parasitology 139: 630-640.

Mao, H., C. Zhu, D. Zong, C. Weng, X. Yang, *et al*., 2015 The Nrde Pathway Mediates Small-RNA-Directed Histone H3 Lysine 27 Trimethylation in *Caenorhabditis elegans*. Curr. Biol. 25: 2398-2403.

Mao, Y. B., W. J. Cai, J. W. Wang, G. J. Hong, X. Y. Tao, *et al*., 2007 Silencing a cotton bollworm P450 monooxygenase gene by plant-mediated RNAi impairs larval tolerance of gossypol. Nat. Biotechnol. 25: 1307–1313.

Napoli, C., C. Lemieux, and R. Jorgensen, 1990 Introduction of a Chimeric Chalcone Synthase Gene into Petunia Results in Reversible Co-Suppression of Homologous Genes in trans. Plant Cell 2: 279-289

Newcombe, R. G., 1998 Two-sided confidence intervals for the single proportion: comparison of seven methods. Statist. Med. 17: 857—872.

Parker, G. S., D. M. Eckert, B. L. Bass, 2006 RDE-4 preferentially binds long dsRNA and its dimerization is necessary for cleavage of dsRNA to siRNA. RNA 12: 807-18.

Pavlidis, P., and W. S. Noble, 2003 Matrix2png: a utility for visualizing matrix data. Bioinformatics 19: 295-296.

Qadota, H., M. Inoue, T. Hikita, M. Köppen, J. D. Hardin, *et al*., 2007 Establishment of a tissue-specific RNAi system in *C. elegans*. Gene 400: 166-173.

Semple, J. I., L. Biondini, and B. Lehner, 2012 Generating transgenic nematodes by bombardment and antibiotic selection. Nat. Methods 9: 118-119.

Sheth, U., J. Pitt, S. Dennis, and J. R. Priess, 2010 Perinuclear P granules are the principal sites of mRNA export in adult *C. elegans* germ cells. Development 137: 1305-1314.

Simmer, F., M. Tijsterman, S. Parrish, S. P. Koushika, M. L. Nonet, *et al.*, 2002 Loss of the putative RNA-directed RNA polymerase RRF-3 makes *C. elegans* hypersensitive to RNAi. Curr. Biol. 12: 1317-9.

Tabara, H., E. Yigit, H. Siomi, C. C. Mello, 2002 The dsRNA binding protein RDE-4 interacts with RDE-1, DCR-1, and a DExH-box helicase to direct RNAi in C. elegans. Cell 109: 861-71.

Tavernarakis, N., S. L. Wang, M. Dorovkov, A. Ryazanov, and M. Driscoll, 2000 Heritable and inducible genetic interference by double-stranded RNA encoded by transgenes. Nat. Genet. 24: 180–183.

Timmons, L., and A. Fire, 1998 Specific interference by ingested dsRNA. Nature 395: 854.

Tomoyasu, Y., S. C. Miller, S. Tomita, M. Schoppmeier, D. Grossmann, *et al.*, 2008 Exploring systemic RNA interference in insects: a genome-wide survey for RNAi genes in Tribolium. Genome Biol. 9: R10.

Winston, W. M., C. Molodowitch, and C. P. Hunter, 2002 Systemic RNAi in *C. elegans* requires the putative transmembrane protein SID-1. Science 295: 2456–2459.

Yigit, E., P. J. Batista, Y. Bei, K. M. Pang, C. C. Chen, *et al*., 2006 Analysis of the *C. elegans* Argonaute Family Reveals that Distinct Argonautes Act Sequentially during RNAi. Cell 127: 747–757.

Yochem, Y., and R.K. Herman, 2003 Investigating *C. elegans* development through mosaic analysis. Development 130: 4761-4768.

Zhang, J., S. A. Khan, C. Hasse, S. Ruf, D. G. Heckel, *et al*., 2015 Full crop protection from an insect pest by expression of long double-stranded RNAs in plastids. Science 347: 991-994.

Zhuang, J. J., and C. P. Hunter, 2011 Tissue Specificity of *Caenorhabditis elegans* Enhanced RNA Interference Mutants. Genetics 188: 235-237.

SUPPLEMENTAL MATERIALS AND METHODS

Strains Used

N2	wild type
AMJ8	*juIs73[Punc-25::gfp] III*
AMJ58	*rde-1(ne219) I; jamEx1[Pmyo-3::rde-1(+)::rde-1 3'UTR & Pmyo-3::DsRed2::unc-54 3'UTR]*
AMJ66	*rde-4(ne301); jamEx4[Pmyo-3::rde-4(+)::rde-4 3'UTR & pHC183]* (same as described in Jose *et al.* 2011 after multiple passages).
AMJ142	*rde-1(ne219) V; rde-4(ne301) III*
AMJ151	*rde-4(ne301); mIs11[Pmyo-2::gfp::unc-54 3'UTR & gut::gfp::unc-54 3'UTR & pes-10::gfp::unc-54 3'UTR] jamIs3[Pmyo-2:DsRed::unc-54 3'UTR] jamIs4[Pmyo-3::rde-4(+)::rde-4 3'UTR & pHC183)] II* (Outcrossed to AMJ8)
AMJ162	*rde-4(ne301); jamEx24[Pnas-9::rde-4(+)::rde-4 3'UTR & Pnas-9::gfp::unc-54 3'UTR]*
AMJ183	*rde-4(ne301); nrde-3(tm1116)*
AMJ188	*rde-4(ne301); jamEx3[Prgef-1::rde-4(+)::rde-4 3'UTR & Prgef-1::gfp::unc-54 3'UTR]*
AMJ190	*rde-4(ne301) III; oxSi221 [Peft-3p::gfp + cb-unc-119(+)] II*
AMJ210	*jamEx24[Pnas-9::rde-4(+)::rde-4 3'UTR & Pnas-9::gfp::unc-54 3'UTR]*
AMJ212	*rde-4(ne301) III; jamEx47[Pwrt-2::rde-4(+)::rde-4 3'UTR & Pwrt-2::gfp::unc-54 3'UTR]*

AMJ217 *rde-4(ne301) III; jamEx52[Punc-54::rde-4(+)::rde-4 3'UTR & Punc-54::gfp::unc-54 3'UTR]*

AMJ220 *rde-4(ne301) III; jamEx55[Psid-2::rde-4(+)::rde-4 3'UTR & Psid-2::gfp::unc-54 3'UTR]*

AMJ229 *rde-4(ne301) III; oxSi221 II; jamEx4*

AMJ237 *rde-4(ne301) III; jamEx65[Pmyo-3::rde-4(+)::rde-4 3'UTR & Pmyo-3::gfp::unc-54 3'UTR]*

AMJ238 *rde-4(ne301) III; jamEx66[Pmyo-3::rde-4(+)::rde-4 3'UTR & Pmyo-3::gfp::unc-54 3'UTR]*

AMJ239 *rde-4(ne301) III; jamEx67[Pmyo-3::rde-4(+)::rde-4 3'UTR & Pmyo-3::gfp::unc-54 3'UTR]*

AMJ290 *rde-4(ne301) III; jamEx89 [Punc-119c::rde-4(+)::rde-4 3'UTR & Punc-119c::gfp::unc-54 3'UTR)]*

AMJ303 *jamEx77 [Pnas-9::gfp::unc-54 3'UTR]*

AMJ314 *oxSi221 II; unc-119(ed3) III (?); rde-1(ne219) V*

AMJ315 *rde-4(ne301) III; mIs11 jamIs3 jamIs4 IV; nrde-3(tm1116) X*

AMJ331 *oxSi221 II; unc-119(ed3) III (?); rde-1(ne219) V; jamEx1*

AMJ383 *eri-1(mg366) IV; jamEx77*

AMJ384 *eri-1(mg366) IV; nrde-3(tm1116) X; jamEx77*

AMJ385 *nrde-3(tm1116) X; jamEx77*

AMJ422 *jamSi6 [Pnas-9::rde-4(+)::rde-4 3'UTR] II; unc-119(ed3) III (?)* (generated by Julia Marré, Jose lab)

AMJ488	*ergo-1(tm1860) V; jamEx77*
AMJ494	*rde-4(ne301) III; nrde-3(tm1116) X; jamEx3*
AMJ495	*rde-4(ne301) III; nrde-3(tm1116) X; jamEx55*
AMJ565	*jamSi6 II; rde-4(ne301) III; unc-119(ed3) III (?)*
AMJ611	*jamSi6 II; unc-119(ed3) III (?) rde-4(ne301) III; nrde-3(tm1116) V*
AMJ612	*rde-4(ne301) III; eri-1(mg366) IV; nrde-3(tm1116) V*
AMJ616	*rrf-1(ok589) I; rde-4(ne301) III [2x outcrossed]*
AMJ617	*rrf-1(ok589) I; rde-4(ne301) III; jamEx3*
AMJ618	*rde-4(ne301) III; rde-1(ne219) V; jamEx3*
AMJ699	*rde-4(ne301) III; mIs11 jamIs3 jamIs4 IV; jamEx77*
AMJ749	*bli-1(jam14) II*
AMJ750	*rde-4(ne301) III; unc-119(ed3) III (?); stIs10226; itIs37*
AMJ783	*jamEx194 [Pmyo-3::DsRed::unc-54 3'UTR]* – line 1
AMJ784	*jamEx195 [Pmyo-3::DsRed::unc-54 3'UTR]* – line 2
AMJ785	*jamEx196 [Pmyo-3::DsRed::unc-54 3'UTR]* – line 3
AMJ788	*rde-1(ne219) V; jamEx199[Psid-2::rde-1(+)::rde-1 3'UTR & Psid-2::gfp::unc-54 3'UTR]*
AMJ793	*jamEx203 [Prgef-1::bli-1-dsRNA & Prgef-1::gfp::unc-54 3'UTR]*
AMJ804	*rde-4(ne301) III; K08F4.2(K08F4.2::gfp) IV*
AMJ805	*oxSi221 II; unc-119(ed3) III(?); jamEx196*
AMJ806	*rde-4(ne301) III; nrIs20 IV; jamEx204 [Psur-5::rde-4(+)::rde-4 3'UTR & Psur-5::DsRed]*

AMJ821	*nrde-3(tm1116) X*; *jamEx203*
AMJ822	*sid-1(qt9) V; jamEx203*
AMJ824	*rde-4(ne301) III; K08F4.2(K08F4.2::gfp) IV; jamEx4*
AMJ825	*rde-4(ne301) III; K08F4.2(K08F4.2::gfp) IV; jamEx3*
AMJ829	*rde-4(ne301) unc-119(ed3) (?) III; stIs10226; itIs37 IV; jamEx52*
AMJ830	*rde-4(ne301) unc-119(ed3) (?) III; stIs10226; itIs37 IV; jamEx3*
EG6070	*oxSi221 II; unc-119(ed3) III*
GR1373	*eri-1(mg366) IV*
HC195	*nrIs20 IV [Pur-5::sur-5::gfp::sur-5 3'UTR]*
HC737	*rde-4(ne301) III; nrIs20 IV*
HC780	*rrf-1(ok589) I*
JH3197	*K08F4.2(K08F4.2::gfp) IV*
RW10226	*unc-119(ed3) III; stIs10226 [Phis-72::HIS-24::mCherry let-858 3' UTR + unc-119(+)]; itIs37 [pie-1 mCherry::H2B-pie-1UTR + unc-119(+)] IV*
WM27	*rde-1(ne219) V*
WM49	*rde-4(ne301) III*
WM156	*nrde-3(tm1116) X*
WM158	*ergo-1(tm1860) V*
YY160	*nrde-1(gg88) III*
YY186	*nrde-2(gg91) II*
YY453	*nrde-4(gg129) IV*

Transgenesis

To express *rde-4(+)* in the body-wall muscle under the *myo-3* promoter:

The wild-type *rde-4* gene was expressed under the control of the *myo-3* promoter from extrachromosomal arrays (AMJ66 (Jose *et al.* 2011), AMJ237, AMJ238, and AMJ239) or from an integrated array (AMJ151)).

Expression from extrachromosomal arrays: To make *Pmyo-3::rde-4(+)::rde-4 3'UTR*, the *myo-3* promoter (*Pmyo-3*) was amplified with primers P28 and P31, and *rde-4(+)* was amplified with primers P30 and P4. The two PCR products were used as templates to generate the *Pmyo-3::rde-4(+)* fusion product with primers P29 and P32. To make *Pmyo-3::gfp::unc-54 3'UTR*, gDNA from a strain with a transgene that expresses *Pmyo-3::gfp::unc-54 3'UTR* (HC150 (*ccIs4251 [pSAK2 (Pmyo-3::nlsGFP-LacZ) & pSAK4 (Pmyo-3::mitoGFP), & dpy-20 subclone)] I; qtIs3 [pBMW14(Pmyo-2::GFP--unc-22--PFG)] III; mIs11 [Pmyo-2::gfp, gut::gfp, pes-10::gfp] IV sid(qt25)*) was used as templates to directly amplify the fusion product with the primers P33 and P34 using Long-Template Expand Polymerase (Roche). WM49 animals were microinjected with a 1:1 mixture (10 ng/µl) of *Pmyo-3::rde-4(+)::rde-4 3'UTR* and *Pmyo-3::gfp::unc-54 3'UTR* in 10 mM Tris (pH 8.5) to generate three independent transgenic lines (AMJ237, AMJ238, and AMJ239).

Expression from an integrated array: A strain with two spontaneous integration events that generated *jamIs3* and *jamIs4* was designated as AMJ151 (*rde-4(ne301) III; mIs11 jamIs3 jamIs4 IV*). Microinjection of pHC448 at 38 ng/µl in 10 mM Tris (pH 8.5) into *rde-4(ne301) III; mIs11* generated *jamIs3*. Subsequent microinjection of a mix of

Pmyo-3::rde-4 and pHC183 (as described earlier in Jose *et al.* 2011) generated *jamIs4*. The resultant strain was then outcrossed by mating with AMJ8 (*juIs73*) to generate *juIs73*/*rde-4(ne301)* heterozygotes and picking their self progeny that lack *juIs73*.

To express *rde-4(+)* in the body-wall muscle under the *unc-54* promoter:

To make *Punc-54::rde-4(+)::rde-4 3'UTR*, the *unc-54* promoter (*Punc-54*) was amplified with primers P22 and P24, and *rde-4(+)* and *rde-4 3'UTR* was amplified with primers P23 and P4. The two PCR products were used as templates to generate the *Punc-54::rde-4(+)::rde-4 3'UTR* fusion product with primers P25 and P5. To make *Punc-54::gfp::unc-54 3'UTR*, *Punc-54* was amplified using primers P22 and P27 and *gfp::unc-54 3'UTR* was amplified from pPD95.75 using primers P26 and P8. The two PCR products were used as templates and *Punc-54::gfp::unc-54 3'UTR* fusion product was generated using the primers P25 and P13. WM49 animals were microinjected with a 1:1 mixture (10 ng/μl) of *Punc-54::rde-4(+)::rde-4 3'UTR* and *Punc-54::gfp::unc-54 3'UTR* in 10 mM Tris (pH 8.5) to generate transgenic lines. A representative transgenic line was designated as AMJ217.

To express *rde-4(+)* in the hypodermis under the *nas-9* promoter:

To make *Pnas-9::rde-4(+)::rde-4 3'UTR*, the *nas-9* promoter (*Pnas-9*) was amplified using the primers P1 and P3, and *rde-4(+)* and *rde-4 3'UTR* was amplified using the primers P2 and P4. The two PCR products were used as templates to generate the *Pnas-9::rde-4(+)::rde-4 3'UTR* fusion product with primers P40 and P5. To make *Pnas-9::gfp::unc-54 3'UTR*, *Pnas-9* was amplified with primers P1 and P7, and *gfp::unc-54 3'UTR* was amplified from pPD95.75 using the primers P6 and P8. WM49 animals were

microinjected with a 2:1:1 mixture of *Pnas-9::rde-4(+)::rde-4 3'UTR* (10 ng/μl), *Pnas-9* (with *gfp* overlap) (5 ng/μl) and *gfp* (with *Pnas-9* overlap) (5 ng/μl) in 10 mM Tris (pH 8.5) to generate transgenic lines. A representative transgenic line was designated as AMJ162.

To make strain AMJ210, AMJ162 was crossed with AMJ8 males. F2 cross progeny that were homozygous for *juIs73* (which is linked to *rde-4(+)*) and contained the *jamEx24[Pnas-9::rde-4(+)::rde-4 3'UTR & Pnas-9::gfp::unc-54 3'UTR]* transgene were passaged for one generation to ensure homozygosity of *juIs73* and then crossed with N2 males. A representative F2 progeny of this cross that lacked *juIs73* (i.e. was homozygous for *rde-4(+)*) but contained the *jamEx24[Pnas-9::rde-4(+)::rde-4 3'UTR & Pnas-9::gfp::unc-54 3'UTR]* transgene was designated as AMJ210.

To express *rde-4(+)* in the hypodermis under the *wrt-2* promoter:

To make *Pwrt-2::rde-4(+)::rde-4 3'UTR*, the *wrt-2* promoter (*Pwrt-2*) was amplified using the primers P9 and P11, and *rde-4(+)::rde-4 3'UTR* was amplified using the primers P10 and P4. The two PCR products were used as templates to generate the *Pwrt-2::rde-4(+)::rde-4 3'UTR* fusion product with primers P12 and P5. To make *Pwrt-2::gfp::unc-54 3'UTR*, *Pwrt-2* was amplified using primers P9 and P15, and *gfp::unc-54 3'UTR* was amplified from pPD95.75 using primers P14 and P8. The two PCR products were used as templates to generate *Pwrt-2*::*gfp* fusion product with primers P12 and P13. WM49 animals were microinjected with a 1:1 mixture (10 ng/μl) of *Pwrt-2::rde-4(+)::rde-4 3'UTR* and *Pwrt-2::gfp::unc-54 3'UTR* in 10 mM Tris (pH 8.5) to generate transgenic lines. A representative transgenic line was designated as AMJ212.

This strain grew slowly for the first ~4 generations, but became comparable to other strains in later generations.

To express *rde-4(+)* in the intestine under the *sid-2* promoter:

To make *Psid-2::rde-4(+)::rde-4 3'UTR*, the *sid-2* promoter (*Psid-2*) was amplified using the primers P16 and P18, and *rde-4(+)* along with *rde-4* 3'UTR was amplified using the primers P17 and P4. The two PCR products were used as templates and the *Psid-2::rde-4(+)::rde-4 3'UTR* fusion product was generated using the primers P19 and P5. To make *Psid-2::gfp::unc-54 3'UTR*, *Psid-2* was amplified using the primers P16 and P21, and *gfp::unc-54 3'UTR* was amplified from pPD95.75 using the primers P20 and P8. The two PCR products were used as template and the *Psid-2::gfp::unc-54 3'UTR* fusion product was generated using the primers P19 and P13. WM49 animals were microinjected with a 1:1 mixture (10 ng/μl) of *Psid-2::rde-4(+)::rde-4 3'UTR* and *Psid-2::gfp::unc-54 3'UTR* in 10 mM Tris (pH 8.5) to generate transgenic lines. A representative transgenic line was designated as AMJ220.

To express *rde-4(+)* in the neurons under the *rgef-1* promoter:

rde-4(ne301); qtEx136; jamEx3[Prgef-1::rde-4(+)::rde-4 3'UTR & Prgef-1::gfp::unc-54 3'UTR] animals (described in Jose *et al.* 2011) were crossed with WM49 and *rde-4(ne301); jamEx3[Prgef-1::rde-4(+)::rde-4 3'UTR & Prgef-1::gfp::unc-54 3'UTR]* progeny were isolated and designated as AMJ188.

To express *rde-4(+)* in the neurons under the *unc-119* promoter:

To make *Punc-119::rde-4(+)::rde-4 3'UTR*, the *unc-119* promoter (*Punc119*) was amplified using the primers P39 and P35, and *rde-4(+)::rde-4 3'UTR* was amplified

using the primers P38 and P4. The two PCR products were used as templates to generate the *Punc-119::rde-4(+)::rde-4 3'UTR* fusion product with primers P41 and P5. To make *Punc-119::gfp::unc-54 3'UTR*, *Punc119* was amplified using primers P39 and P36, and *gfp::unc-54 3'UTR* was amplified from pBH34.21 using the primers P37 and P42. The two PCR products were used as templates and the *Punc-119::gfp::unc-54 3'UTR* fusion product was generated using the primers P41 and P43. WM49 animals were microinjected with a 1:1 mixture (10 ng/μl) of *Punc-119::rde-4(+)::rde-4 3'UTR* and *Punc-119::gfp::unc-54 3'UTR* in 10 mM Tris (pH 8.5) to generate transgenic lines. A representative transgenic line was designated as AMJ290.

To express *rde-1(+)* in the body-wall muscles under the *myo-3* promoter:

As described in Jose *et al.* 2011.

To express *rde-1(+)* in the intestine under the *sid-2* promoter:

To make *Psid-2::rde-1(+)::rde-1 3'UTR*, the *sid-2* promoter (*Psid-2*) was amplified using the primers P16 and P72, and *rde-1(+)::rde-1 3'UTR* was amplified using the primers P73 and P46. The two PCR products were used as templates to generate the *Psid-2::rde-1(+)::rde-1 3'UTR* fusion product with primers P19 and P47. Coinjection marker *Psid-2::gfp::unc-54 3'UTR*, was made as described for AMJ220. WM27 animals were microinjected with a 1:1 mixture (10 ng/μl) of *Psid-2::rde-1(+)::rde-1 3'UTR* and *Psid-2::gfp::unc-54 3'UTR* in 10 mM Tris (pH 8.5) to generate transgenic lines. A representative transgenic line was designated as AMJ788.

To express *rde-1(+)* in the hypodermis under the *wrt-2* promoter:

To make *Pwrt-2::rde-1(+)::rde-1 3'UTR*, the *wrt-2* promoter (*Pwrt-2*) was amplified using the primers P9 and P43, and *rde-1(+)::rde-1 3'UTR* was amplified using the primers P44 and P46. The two PCR products were used as templates to generate the *Pwrt-2::rde-1(+)::rde-1 3'UTR* fusion product with primers P12 and P47. *Pwrt-2::gfp::unc-54 3'UTR* was made as described for AMJ212. WM27 animals were microinjected with a 1:1 mixture (10 ng/μl) of *Pwrt-2::rde-1(+)::rde-1 3'UTR* and *Pwrt-2::gfp::unc-54 3'UTR* in 10 mM Tris (pH 8.5) to generate transgenic lines. Three representative transgenic lines were designated as AMJ631, AMJ632, and AMJ633.

To express *rde-1(+)* in neurons under the *rgef-1* promoter:

Made as described in Jose *et al.* 2011.

To express *rde-4(+)* in all somatic nuclei under the *sur-5* promoter:

To make *Psur-5::rde-4(+)::rde-4 3'UTR*, the *sur-5* promoter (*Psur-5*) was amplified using the primers P74 and P75, and *rde-4(+)* along with *rde-4* 3'UTR was amplified using the primers P76 and P4. The two PCR products were used as templates and the *Psur-5::rde-4(+)::rde-4 3'UTR* fusion product was generated using the primers P77 and P5. To make *Psur-5::DsRed*, *Psur-5* was amplified using the primers P74 and P78, and nuclear localized *DsRed* was amplified from pGC306 using the primers P79 and P80. The two PCR products were used as template and the *Psur-5::DsRed* fusion product was generated using the primers P77 and P81. HC737 animals were microinjected with a 1:1 mixture (10 ng/μl) of *Psur-5::rde-4(+)::rde-4 3'UTR* and *Psur-5::DsRed::unc-54 3'UTR* in 10 mM Tris (pH 8.5) to generate transgenic lines. A representative transgenic line was designated as AMJ806.

To express *gfp* in the hypodermis under the *nas-9* promoter:

To make *Pnas-9::gfp::unc-54 3'UTR*, the *nas-9* promoter (*Pnas-9*) was amplified with primers P1 and P6, and *gfp::unc-54 3'UTR* was amplified from pPD95.75 using primers P48 and P8. The two PCR products were used as templates and *Pnas-9::gfp::unc-54 3'UTR* fusion product was generated using the primers P40 and P13. N2 animals were microinjected with a *Pnas-9::gfp::unc-54 3'UTR* in 10 mM Tris (pH 8.5) to generate transgenic lines. A representative transgenic line was designated as AMJ303.

To express *DsRed* in the body-wall muscle under the *myo-3* promoter:

N2 animals were microinjected with pHC183 (*Pmyo-3::DsRed::unc-54 3'UTR,* made as described in Jose *et al.* 2011) in 10 mM Tris (pH 8.5) to generate 3 transgenic lines designated as AMJ783, AMJ784 and AMJ785.

To express *rde-4(+)* in the hypodermis under the *nas-9* promoter from a single-copy transgene:

EG4322 animals were microinjected with a mixture of pJM6 (22.5ng/µl) and the coinjection markers pCFJ601 (50ng/µl), pMA122 (10 ng/µl), pGH8 (10 ng/µl), pCFJ90 (2.5 ng/µl), and pCFJ104 (5 ng/µl) (plasmids described in Semple *et al.* 2012) to generate a transgenic line as described earlier (Semple *et al.* 2012). This isolated line was crossed into AMJ8 males and *rde-4(-)/juIs73* male progeny were crossed to WM49 background to generate AMJ565. The integration of *Pnas-9::rde-4(+)::rde-4 3'UTR* in AMJ565 was verified by genotyping for the presence of *Pnas-9::rde-4(+)* using primers P54 and P55.

To express *bli-1-dsRNA* in the neurons under the *rgef-1* promoter:

To make *Prgef-1::bli-1-dsRNA* sense strand, the *rgef-1* promoter (*Prgef-1*) was amplified with primers P84 and P85 and a 1kb region in exon 3 of *bli-1* was amplified using primers P86 and P87. The two PCR products were used as templates and *Prgef-1::bli-1-dsRNA* sense fusion product was generated using the primers P88 and P89. To make *Prgef-1::bli-1-dsRNA* antisense strand, the *rgef-1* promoter (*Prgef-1*) was amplified with primers P84 and P90 and *bli-1* was amplified using primers P91 and P92. The two PCR products were used as templates and *Prgef-1::bli-1-dsRNA* antisense fusion product was generated using the primers P88 and P93. N2 animals were microinjected with a 1:1:1 ratio of sense *Prgef-1::bli-1-dsRNA,* antisense *Prgef-1::bli-1-dsRNA* and *Prgef-1::gfp::unc-54 3'UTR* (as described in Jose *et al*. 2011) in 10 mM Tris (pH 8.5) to generate transgenic lines. A representative transgenic line was designated as AMJ793.

SUPPLEMENTAL FIGURES AND FIGURE LEGENDS

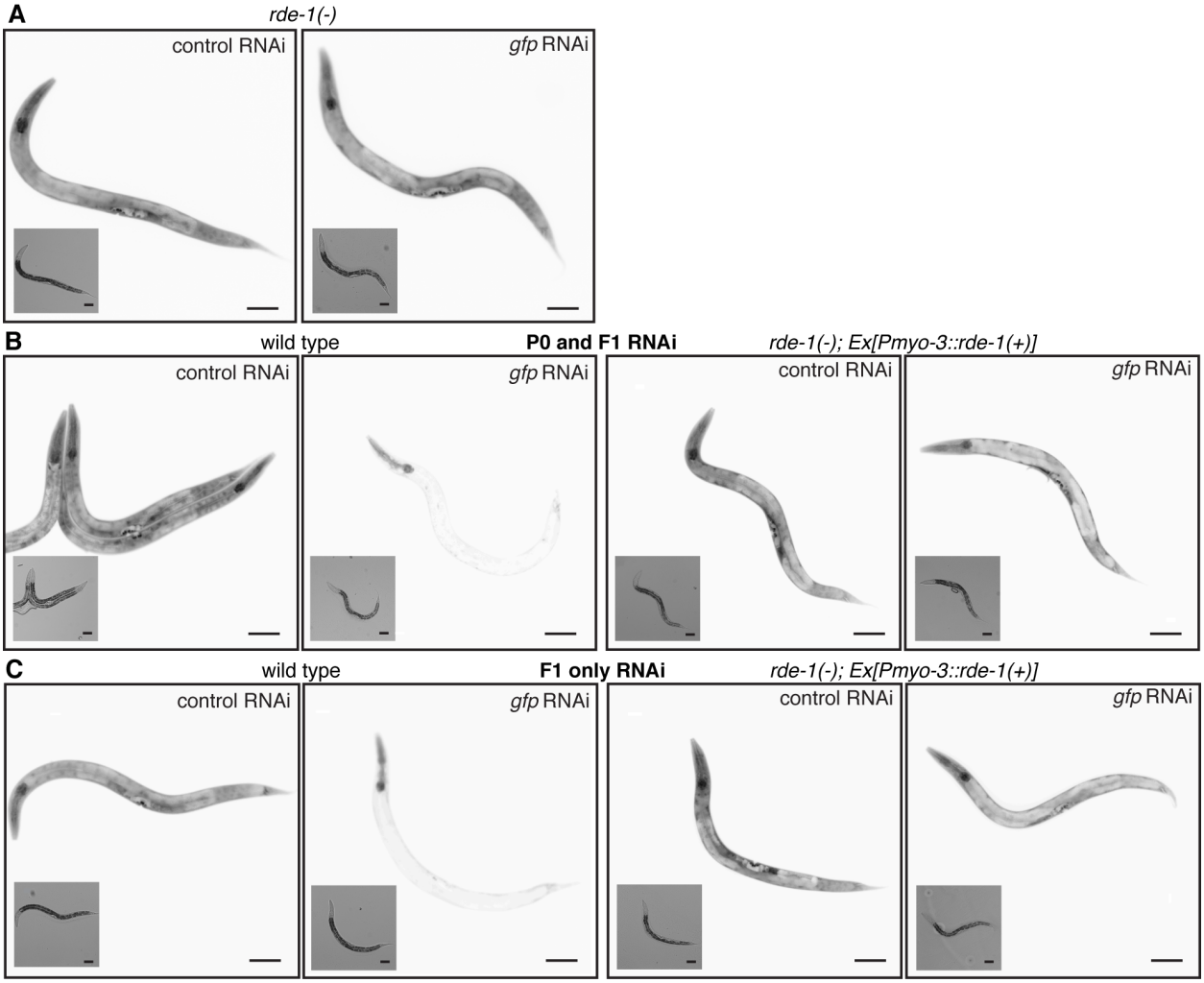

Figure S1. Expression of RDE-1 under the *myo-3* promoter enables weak silencing of *gfp* in *rde-1(-)* tissues. Representative images of *rde-1(-)* animals (A) or *rde-1(-)* animals with *rde-1(+)* expressed in the muscle (*rde-1(-); Ex[Pmyo-3::rde-1(+)]*, *right*) that were fed control RNAi or *gfp* RNAi for two generations (P0 and F1 RNAi in B) or for one generation (F1 only RNAi in A) are shown. Insets are brightfield images, scale bar = 50 μm. Also see File S1.

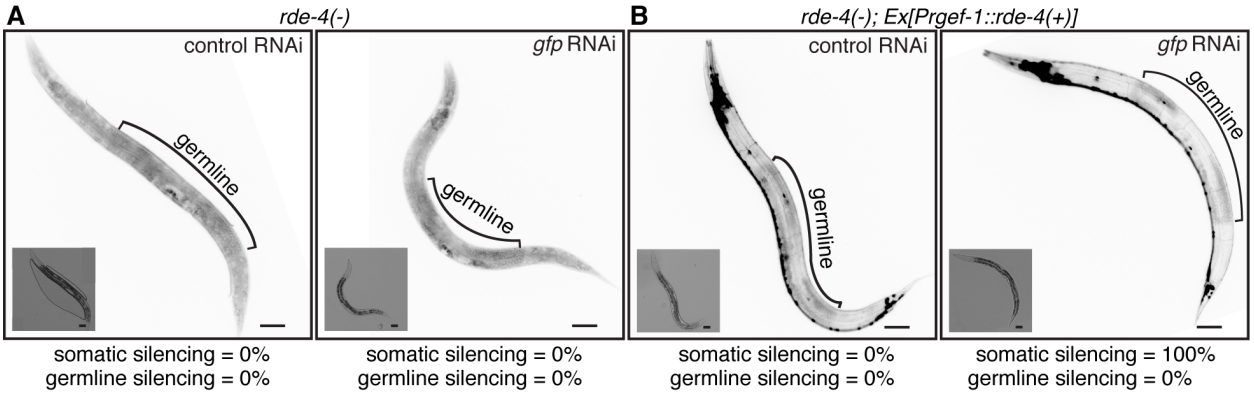

Figure S2. Neuronal rescue of *rde-4* enables silencing of *gfp* in *rde-4(-)* somatic tissue but not in *rde-4(-)* germline. Representative images of animals with *gfp* expression in all somatic and germline cells (*Pgtbp-1::gtbp-1::gfp*) in a *rde-4(-)* background (A), or *rde-4(-)* background with *rde-4(+)* expressed in neurons (B, *Ex[Prgef-1::rde-4(+)*) that were fed either control RNAi (*left*) or *gfp* RNAi (*right*) are shown. Percentages of animals showing silencing in somatic cells and germline are indicated. Insets are brightfield images, scale bar = 50 μm, and n = 50 L4-staged animals. Also see Figure 1B&C and File S1.

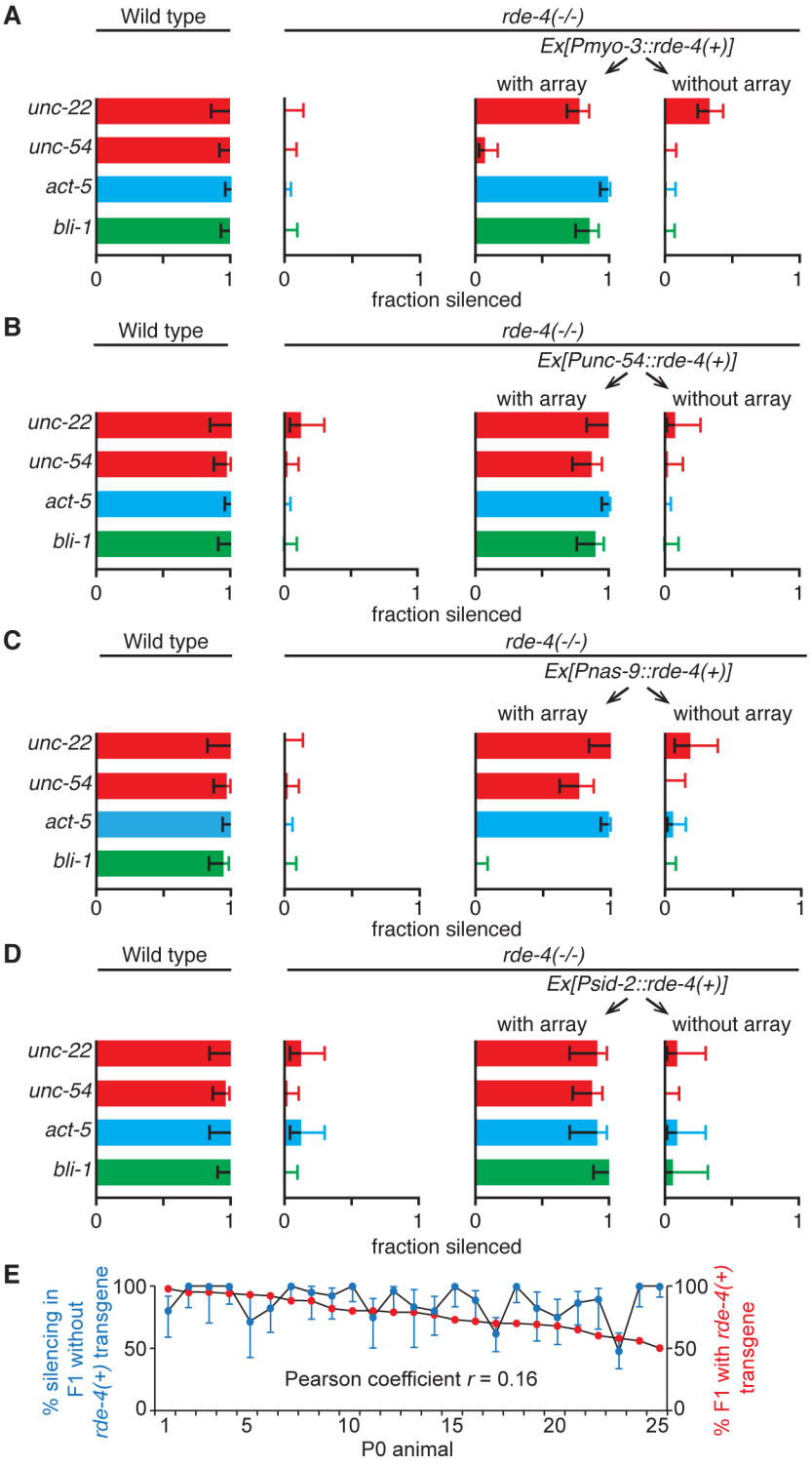

Figure S3. Expression of RDE-4 in parental soma does not usually enable silencing by feeding RNAi in *rde-4(-)* progeny. (A-D) Progeny of wild-type animals,

rde-4(-) animals, or *rde-4(-)* animals expressing *rde-4(+)* in the muscle (*Pmyo-3* or *Punc-54*), hypodermis (*Pnas-9*), or intestine (*Psid-2*) were fed dsRNA against *unc-22*, *unc-54*, *act-5* or *bli-1* and the fractions of animals that showed silencing (fraction silenced) were determined. Also see Figure 2A. (E) Extent of silencing upon feeding RNAi against *unc-22* in *rde-4(-)* progeny of animals with an extrachromosomal *Pmyo-3::rde-4(+)* transgene is not correlated with the rate of transmission of the transgene from parent to progeny. Silencing (% silencing in F1 without *rde-4(+)* transgene) and transmittance (% F1 with *rde-4(+)* transgene) were measured in progeny (F1) of 25 animals with the extrachromosomal array (P0 animal). Error bars indicate 95% CI and n>15 F1 animals.

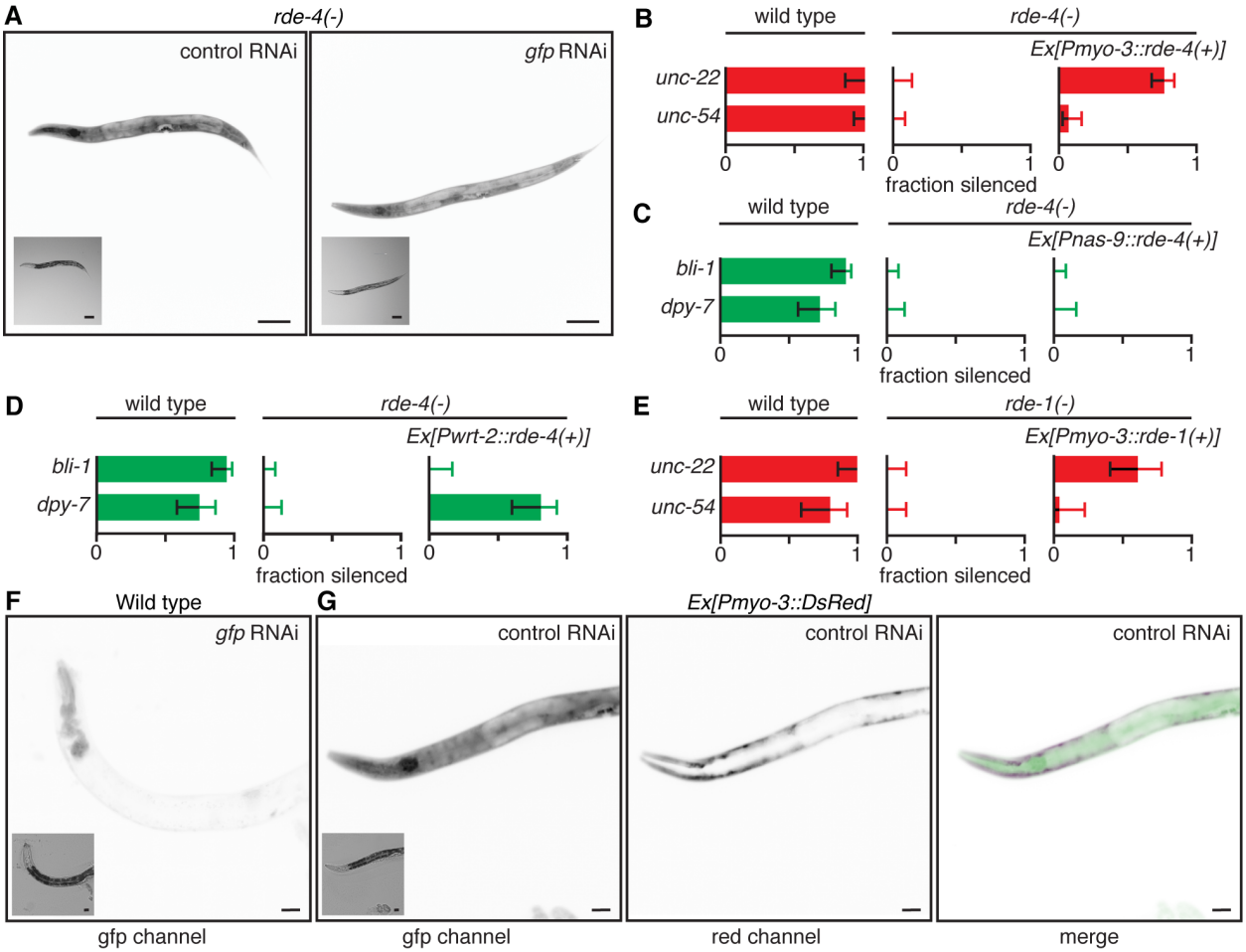

Figure S4. Silencing by feeding RNAi of some genes is reduced in tissues expressing RDE-4 or RDE-1 from a repetitive transgene. (A) Silencing by feeding RNAi of *gfp* expressed from a single-copy transgene in all somatic cells requires *rde-4*. Representative images of a *rde-4(-)* animal that express *gfp* in all somatic cells and were fed either control dsRNA (control RNAi, *left*) or dsRNA against *gfp* (*gfp* RNAi, *right*) are shown. Insets are brightfield images, scale bar = 50 μm. Also see Figure 4A&B and File S1. (B-E) Silencing by feeding RNAi of some endogenous genes is reduced in tissues expressing *rde-4(+)* or *rde-1(+)* from a repetitive transgene. Wild-type animals, mutant animals (*rde-4(-)* in B,C,D or *rde-1(-)* in E) or mutant animals with tissue specific rescues in the body-wall muscles (*Pmyo-3* in B and E) or hypodermis (*Pnas-9* in C or *Pwrt-2* in D) were fed dsRNA against *unc-22*, *unc-54*, *bli-1*, or *dpy-7* and the fractions of animals that showed silencing (fraction silenced) were determined. Error bars indicate 95% CI and n>24 animals. (F, G) Representative images of animals with *gfp* expression in all somatic cells that were fed *gfp* RNAi (F) or animals that in addition express *DsRed* in the body-wall muscle (*Pmyo-3::DsRed*) that were fed control RNAi (G) are shown. Merged images in (G) show overlap of *gfp* and *DsRed* expression (red channel = magenta; green channel = green; and merge = black). Insets are brightfield images and scale bar = 50 μm. Also see Figure 4D, E.

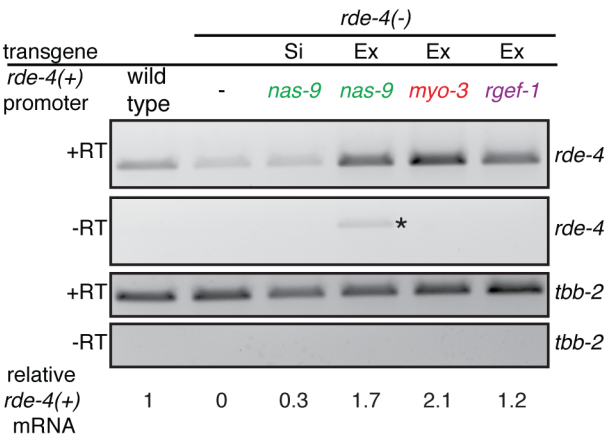

Figure S5. Animals expressing *rde-4(+)* from repetitive transgenes express higher levels of *rde-4(+)* mRNA compared to animals expressing *rde-4(+)* from a single-copy transgene. Semiquantitative RT-PCR of *rde-4* mRNA and *tbb-2* mRNA (control) in wild-type animals, *rde-4(-)* animals, or *rde-4(-)* animals expressing *rde-4(+)* using a repetitive transgene (*Ex(nas-9)*, *Ex(myo-3)*, or *Ex(rgef-1)*) or a single-copy transgene (*Si(nas-9)*). Levels of *rde-4(+)* mRNA relative to that in wild-type animals are indicated for each strain. Asterisk indicates band corresponding to genomic DNA.

B

# injected (growth)	Total F1s scored	Rol(%)	DpyRol(%)	Dpy(%)	Bli(%)				
					Total(%)	Wt(%)	Rol(%)	DpyRol(%)	Dpy(%)
4 (20°C)	239	15.5	2.5	3.8	2.9	0	28.6	0	71.4
	121	24	2.4	18.2	9.1	81.8	0	0	18.2
	204	15.2	1.5	6.9	6.9	50	21.4	0	28.6
	157	20.4	6.4	10.8	8.9	57.1	28.6	0	14.3
4 (15°C)	225	11.1	1.8	3.6	2.7	16.7	66.7	16.7	0
	166	9	1.8	8.4	2.4	75	25	0	0
	165	10.9	1.8	7.3	3.6	0	83.3	0	16.7
	261	14.2	1.9	6.1	3.1	50	37.5	12.5	0

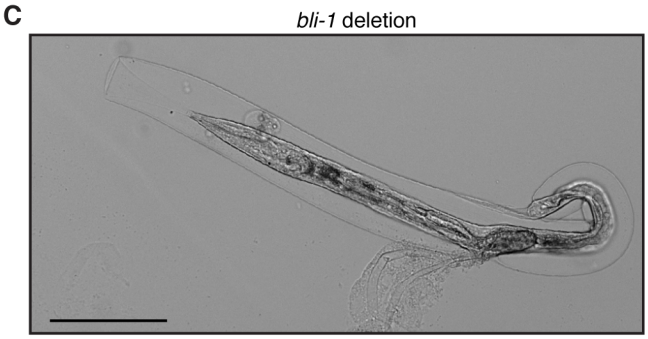

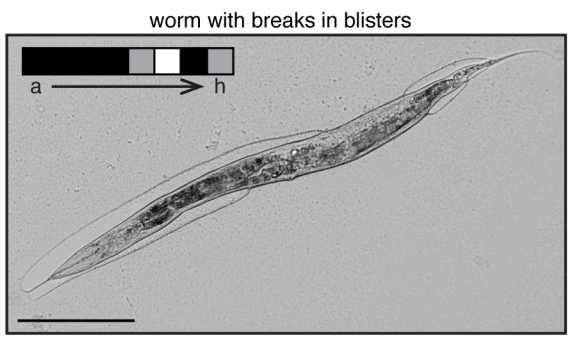

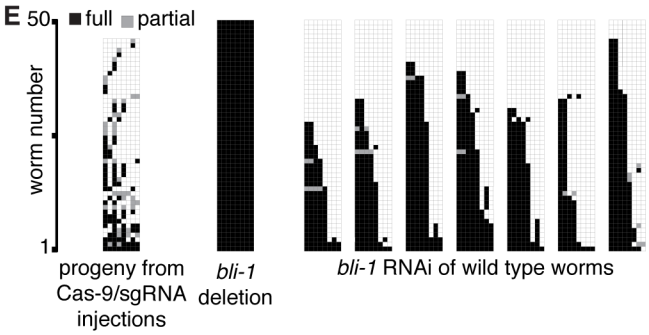

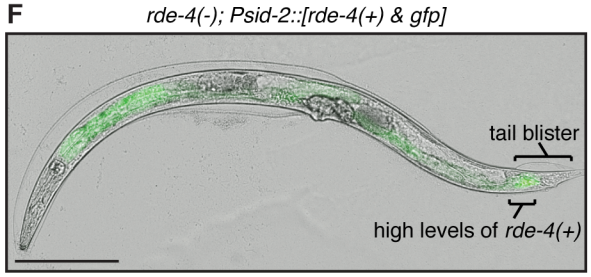

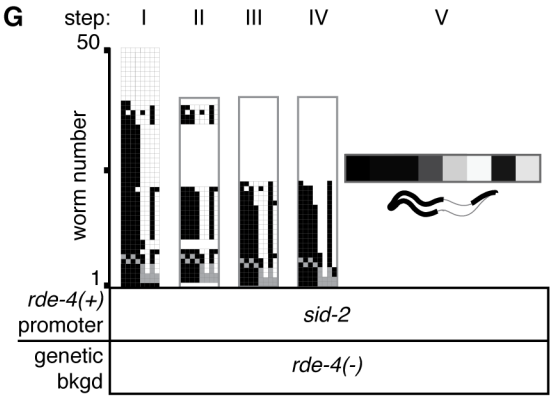

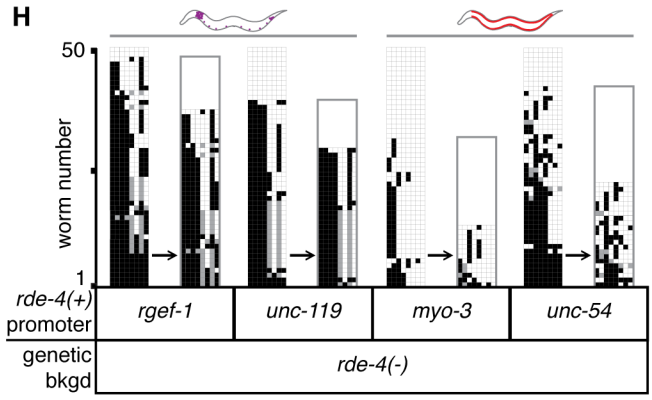

Figure S6. Silencing of *bli-1* upon feeding RNAi in animals with tissue-specific rescue of *rde-4* in non-hypodermal cells results in unique patterns of blisters that differ from those in *bli-1(-)* animals. (A) Design of Cas9-based genome editing to generate a *bli-1* null mutant. The *bli-1* gene (exons, blue boxes; introns, grey lines) was targeted by a single-guide RNA (sgRNA) that cuts within the gene (orange *) and was repaired with a double-stranded DNA template (green flanking the gene). (B) Results from Cas9/sgRNA injection into wild-type worms to generate a *bli-1* null mutant. Wild-type animals were simultaneously targeted for edits in *dpy-10* and *bli-1* (co-conversion strategy (Arribere *et al.* 2014)), resulting in progeny that displayed Rol, DpyRol and Dpy defects (indicative of *dpy-10* editing) with or without blisters as indicated. (C) Null mutations in *bli-1* result in blisters that cover the entire body. A representative image of a *bli-1* null mutant animal generated by Cas9-based genome editing. Scale bar = 50 μm. (D) A representative animal to illustrate scoring of *bli-1* silencing in each section of the worm. The animal was divided into 8 sections (a through h, see Figure 6A) and each section was scored for presence of a full blister (black), partial blister (grey), or no blister (white) as indicated in the inset. Scale bar = 50 μm. (E) Wild-type animals display a stereotyped pattern of susceptibility to *bli-1* feeding RNAi. Progeny of wild-type animals targeted by Cas9-based genome editing, *bli-1* null mutant animals, and wild-type animals exposed to feeding RNAi were scored for blister patterns as described in Figure 6A (n>45 gravid adult animals). Unlike sections in the progeny of animals that were injected with Cas9/sgRNA or in *bli-1* null mutants, sections in wild-type animals that were subject to *bli-1* feeding RNAi showed a stereotyped frequency of blister formation

(a > b > … > h). (F) RDE-4 expression in intestinal cells near the tail correlates with blister formation in *rde-4(-)* hypodermis near the tail upon *bli-1* RNAi. Complete image of animal shown in Figure 6B. (G,H) Blister scoring method to detect variations in the pattern of blister formation upon *bli-1* feeding RNAi. (G) The pattern of blister formation in *rde-4(-)* animals with *rde-4(+)* expressed in the intestine (*Psid-2*) was examined (step I) and animals following the stereotyped order of susceptibility to *bli-1* RNAi (a > b > … > h) were removed (step II). The remaining animals, which show variant susceptibility to *bli-1* feeding RNAi, were aggregated (step III and IV) and collapsed into a heat map (step V) to assess frequency of variant blisters in each section. (H) The pattern of *bli-1* silencing in *rde-4(-)* animals with *rde-4(+)* expressed from neuronal promoters (*Prgef-1 & Punc-119*), body-wall muscle promoters (*Pmyo-3 & Punc-54*) were examined and variant blisters were isolated (n = 50 adult animals).

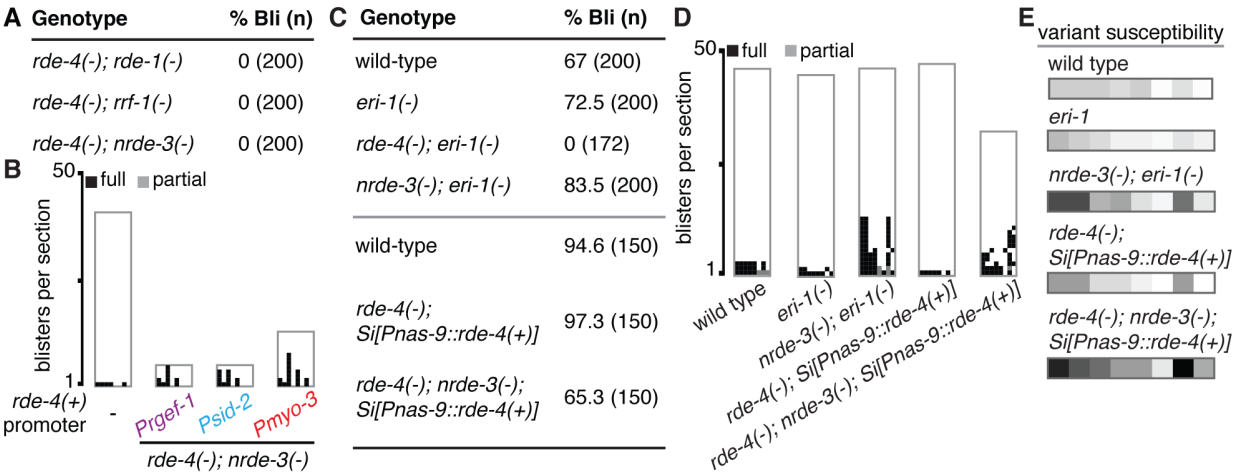

Figure S7. Loss of the exonuclease *eri-1* or transgenic expression of RDE-4 in the hypodermis can bypass the requirement for NRDE-3 to silence *bli-1* in response to ingested dsRNA. (A) Double mutant animals that lack *rde-4* and either *rde-1*, *rrf-1* or *nrde-3* were fed dsRNA against *bli-1* and analyzed as in Figure 7A. (B) Silencing of *bli-1*

by mobile RNA derived from ingested RNA in the absence of *nrde-3* results in similar patterns of blister formation when *rde-4(+)* is expressed in neurons, intestine, or body-wall muscles. Patterns of blister formation in wild-type animals or *rde-4(-); nrde-3(-)* mutant animals with *rde-4(+)* expressed in neurons (*Prgef-1*), intestine (*Psid-2*) or body-wall muscles (*Pmyo-3*) upon *bli-1* feeding RNAi were analyzed and plotted as in Figure 6C. (C-E) Loss of *eri-1* or transgenic expression of *rde-4(+)* in the hypodermis can bypass the requirement of *nrde-3* for silencing *bli-1* by feeding RNAi. (C, top) Wild-type animals, *eri-1(-)* animals, or double mutant animals lacking *eri-1* and either *rde-4* or *nrde-3* were fed dsRNA against *bli-1* and analyzed as in Figure 7A. (C, bottom) Wild-type animals and *rde-4(-)* animals or *rde-4(-); nrde-3(-)* animals expressing *rde-4(+)* in the hypodermis from a single copy transgene (*Si[Pnas-9::rde-4(+)]*) were fed dsRNA against *bli-1* and analyzed as in Figure 7A. (D,E) Patterns of blister formation in animals assayed in C were analyzed in gravid adults (n=50 for D and n=100 for E) and plotted as in Figure 6C,D.

SUPPLEMENTAL TABLES

Table S1. Feeding RNAi and defects scored.

Gene	Expression	Defect scored upon RNAi
unc-22	body-wall muscle	L4 or young adults twitch within 2 minutes in response to 3mM levamisole (Sigma Aldrich).
unc-54	body-wall muscle	Inability to move backwards upon touching the head and lack of sinusoidal movement.
act-5	intestine	Failure to develop to the 4th larval stage in 3 days.

dpy-7	hypodermis	Short, fat L4- or adult-staged animals
bli-1	hypodermis	Presence of fluid-filled blisters on adults
pos-1	germline	Animals that laid >90% unhatched eggs
par-1	germline	Animals that laid >66% unhatched eggs
par-2	germline	Animals that laid >80% unhatched eggs

Table S2. Oligonucleotides used.

Name	Sequence
P1	gttccattcatcggcatgag
P2	ttcatcattctgttcaattcttcatggatttaaccaaactaacg
P3	cgttagtttggttaaatccatgaagaattgaacagaatgatgaa
P4	cactgcagagaatgagtgtg
P5	gtagaggtcagaggcatag
P6	ttcatcattctgttcaattcttcatgagtaaaggagaagaacttttc
P7	gaaaagttcttctcctttactcatgaagaattgaacagaatgatgaa
P8	cggtcataaactgaaacgtaac
P9	tcacggaactgacttcttg
P10	acctgccaattgtttctcggatggatttaaccaaactaacg
P11	cgttagtttggttaaatccatccgagaaacaattggcaggt
P12	ctgacatgcaaatggtgtg
P13	ctgaaacgtaacatatgataagg
P14	acctgccaattgtttctcggatgagtaaaggagaagaacttttc

P15	gaaaagttcttctcctttactcatccgagaaacaattggcaggt
P16	aattggatggatggcttctg
P17	caaaaccctgatattttcaggaaatggatttaaccaaactaacg
P18	cgttagtttggttaaatccatttcctgaaaatatcagggttttg
P19	ctgcctattgggactcaacg
P20	caaaaccctgatattttcaggaaatgagtaaaggagaagaacttttc
P21	gaaaagttcttctcctttactcatttcctgaaaatatcagggttttg
P22	ttgttgccgccaatttgc
P23	ccatttgaaagaagcgagaaatcatggatttaaccaaactaacg
P24	cgttagtttggttaaatccatgatttctcgcttctttcaaatgg
P25	ggtatgagagagtggcagag
P26	ccatttgaaagaagcgagaaatcatgagtaaaggagaagaacttttc
P27	gaaaagttcttctcctttactcatgatttctcgcttctttcaaatgg
P28	aggctgcaacaaagatcagg
P29	tctctccgtacgtgtactctatcactgccggc
P30	cgaccactagatccatctagaaatggatttaaccaaactaacg
P31	cgttagtttggttaaatccatttctagatggatctagtggtcg
P32	agagagctcgaggtagaggtcagaggcatag
P33	ggtcggctataataagttcttg
P34	cggtcataaactgaaacgtaac
P35	cgttagtttggttaaatccatctgaaaaaaaaaagagttttc
P36	gcttcttctttggagcagtcatctgaaaaaaaaaagagttttc

P37	gaaaactctttttttttcagatgactgctccaaagaagaagc
P38	gaaaactctttttttttcagatggatttaaccaaactaacg
P39	gtacaaatgacacagagccg
P40	cttctcgcctctaagaaattc
P41	aaatgacacagagccgacg
P42	ctgaaacgtaacatatgataagg
P43	cggtcataaactgaaacgtaac
P44	tttctcggatgtcctcgaattttcccga
P45	acctgccaattgtttctcggatgtcctcgaattttcccg
P46	gctcaactggagaagtgtga
P47	gcaggtgatttcacgacttc
P48	gaaaagttcttctcctttactcatgaagaattgaacagaatgatg
P49	tgctatgaggcacaggtaac
P50	cgttagtttggttaaatccattgaacagaatgatgaattgcg
P51	cgcaattcatcattctgttcaatggatttaaccaaactaacg
P52	tctctccctgcaggatttcaaatgtggaataaacctgt
P53	gagagaactagtgtagaggtcagaggcatag
P54	ccattgatctttgcccactc
P55	gctttcttgcttgttgcctg
P56	atttaggtgacactatagattactcctggctgacctgttttagagctagaaatagcaag
P57	tggcaccgagtcggtgc
P58	atttaggtgacactatagctaccataggcaccacgaggttttagagctagaaatagcaag

P59	cgctcgtctctcaaattcag
P60	agactagaagtttttttagttagatgaggttagatcacactac
P61	gtagtgtgatctaacctcatctaactaaaaaaaacttctagtct
P62	cccatctttccagatatacc
P63	atatagactgcggtgactgg
P64	tcccttcatgtcttcgcaac
P65	cacttgaacttcaatacggcaagatgagaatgactggaaaccgtaccgcatgcggtgcctatggtagcgga gcttcacatggcttcagaccaacagccta
P66	cagtgtgcttgtaaatcggc
P67	tgctcttcggcagttgcttc
P68	gcaaagaatcttgcagcatgg
P69	gaacacacccagactgaaga
P70	gacgagcaaatgctcaacg
P71	tcgtcttcggcagttgcttc
P72	tcgggaaaattcgaggacatttcctgaaaatatcagggtttt
P73	aaaaccctgatattttcaggaaatgtcctcgaattttcccga
P74	caaggaagaactctgtacgg
P75	aacgttagtttggttaaatccattctgaaaacaaaatgtaaagttca
P76	tgaactttacattttgttttcagaatggatttaaccaaactaacgtt
P77	gaaattgaagacgcaacaaaaac
P78	cttcttctttggagcagtcattctgaaaacaaaatgtaaagttca
P79	tgaactttacattttgttttcagaatgactgctccaaagaagaag

P80	tctcaaggatcttaccgctg
P81	acgcatctgtgcggtatttc
P82	cttctcaccacgctttaccattg
P83	tcgggaaggcttcataggaac
P84	cgataatctcgtgacactcg
P85	gaggaggtgcacggaaaccgtcgtcgtcgtcgatgc
P86	gcatcgacgacgacgacggtttccgtgcacctcctc
P87	tttcttccaggtagtccagg
P88	ccccttatatcagcacac
P89	gttgaccatcttgtccgttc
P90	cctggactacctggaagaaacgtcgtcgtcgtcgatgc
P91	gcatcgacgacgacgacgtttcttccaggtagtccagg
P92	atgcccagaactatccaagg
P93	gtttccgtgcacctcctc

File S1. Unedited images. The file contains a compilation of original raw images of all representative worm images used in the paper. (Fig 1B_1-Fig 1B_2) wild-type animals expressing *Pgtbp-1::gtbp-1::gfp* fed control RNAi (1) or *gfp* RNAi (2). (Fig 1C_1-Fig 1C_4) *rde-4(-); Pmyo-3::rde-4(+)* animals expressing *Pgtbp-1::gtbp-1::gfp* fed control RNAi (1-green channel, 2-red channel) or *gfp* RNAi (3-green channel, 4-red channel). (Fig 3B_1-Fig 3B_2) wild-type animals expressing *Psur-5::sur-5::gfp* fed control RNAi (1) or *gfp* RNAi (2). (Fig 3C_1-Fig 3C_2) *rde-4(-)* animals expressing *Psur-5::sur-5::gfp* fed control RNAi (1) or *gfp* RNAi (2). (Fig 3D_1-Fig 3D_4) *rde-4(-);Psur-5::rde-4(+)&DsRed* animals expressing *Psur-5::sur-5::gfp* fed control RNAi (1-green channel, 3-red channel) or *gfp* RNAi (2-green channel, 4-red channel). (Fig 4A_1-Fig 4A_2) wild-type animals expressing *Peft-3::gfp* fed control RNAi (1) or *gfp* RNAi (2). (Fig 4B_1-Fig 4B_2) *rde-4(-); Pmyo-3::rde-4(+)* animals fed control RNAi (1) or *gfp* RNAi (2). (Fig 4D_1-Fig 4D_2) animals expressing *Pmyo-3::DsRed* fed *gfp* RNAi (1-green channel, 2-red channel). (Fig S1A_1-Fig S1A_2) *rde-1(-)* animals expressing *Peft-3::gfp* fed control RNAi (1) or *gfp* RNAi (2). (Fig S1B_1-Fig S1B_4) P0&F1 RNAi of *Peft-3::gfp* animals in a wild type background (control RNAi (1) or *gfp* RNAi (2)) or in a *rde-4(-); Pmyo-3::rde-4(+)* background fed (control RNAi (3) or *gfp* RNAi (4). (Fig S1C_1-Fig S1C_4) F1-only RNAi of *Peft-3::gfp* animals in a wild type background (control RNAi (1) or *gfp* RNAi (2)) or in a *rde-4(-); Pmyo-3::rde-4(+)* background fed (control RNAi (3) or *gfp* RNAi (4). (Fig S2A_1-Fig S2A_2) *Pgtbp-1::gfp* animals in a wild type background fed control RNAi (1) or *gfp* RNAi (2). (Fig S2B_1-Fig S2B_2) *Pgtbp-1::gfp* animals in a *rde-4(-); Pmyo-3::rde-4(+)* background fed control RNAi (1) or *gfp* RNAi (2). (Fig S4A_1-Fig S4A_2) *rde-4(-)*

animals expressing *Peft-3::gfp* fed control RNAi (1) or *gfp* RNAi (2). (Fig S4F) wild-type animal expressing *Peft-3::gfp* fed *gfp* RNAi. (Fig S4G_1-Fig S4G_2) animals expressing *Pmyo-3::DsRed* fed control RNAi (1-green channel, 2-red channel).